

Tagged Particle Correlations in the Asymmetric Simple Exclusion Process : Finite Size Effects

Shamik Gupta¹, Satya N. Majumdar², Claude Godrèche³, and Mustansir Barma¹

¹*Department of Theoretical Physics,*

Tata Institute of Fundamental Research,

Homi Bhabha Road, Mumbai 400 005, India

²*Laboratoire de Physique Théorique et Modèles Statistiques,*

Université Paris-Sud, Orsay-Cedex, France

³*Service de Physique Théorique, CEA Saclay, France*

(Dated: May 2, 2019)

We study finite size effects in the variance of the displacement of a tagged particle in the stationary state of the Asymmetric Simple Exclusion Process (ASEP) on a ring of size L . The process involves hard core particles undergoing stochastic driven dynamics on a lattice. The variance of the displacement of the tagged particle, averaged with respect to an initial stationary ensemble and stochastic evolution, grows linearly with time at both small and very large times. We find that at intermediate times, it shows oscillations with a well defined size-dependent period. These oscillations arise from sliding density fluctuations (SDF) in the stationary state with respect to the drift of the tagged particle, the density fluctuations being transported through the system by kinematic waves. In the general context of driven diffusive systems, both the Edwards-Wilkinson (EW) and the Kardar-Parisi-Zhang (KPZ) fixed points are unstable with respect to the SDF fixed point, a flow towards which is generated on adding a gradient term to the EW and the KPZ time-evolution equation. We also study tagged particle correlations for a fixed initial configuration, drawn from the stationary ensemble, following earlier work by van Beijeren. We find that the time dependence of this correlation is determined by the dissipation of the density fluctuations. We show that an exactly solvable linearized model captures the essential qualitative features seen in the finite size effects of the tagged particle correlations in the ASEP. Moreover, this linearized model also provides an exact coarse-grained description of two other microscopic models.

PACS numbers: 02.50.Ey, 05.40.-a, 05.60.Cd, 66.30.Dn, 05.50.+q

I. INTRODUCTION

The Asymmetric Simple Exclusion Process (ASEP) is a prototype model to study driven diffusive motion [1]. The process involves hard-core particles hopping between neighboring sites of a lattice, with an asymmetry in hopping rates which incorporates the effect of an external drive. In the case of completely asymmetric dynamics, the ASEP reduces to the totally asymmetric simple exclusion process (TASEP). In either case, the system, on a periodic lattice, settles at long times into a non-equilibrium stationary state in which each particle has an average drift velocity, and there is a finite current through the system.

In this paper, we are interested in the temporal growth of the fluctuations in the displacement of a tagged ASEP particle in the steady state in a *finite* system of size L in one dimension. We monitor the variance $\sigma^2(L, t)$ of a *tagged* particle around its average in time t , starting from the stationary ensemble of configurations. Some asymptotic results are already known [2, 3, 4, 5, 6]. These are summarized below.

(a) On taking the limit $L \rightarrow \infty$ first, followed by the limit $t \rightarrow \infty$, the fluctuations are diffusive, growing linearly in time: $\sigma^2(L, t) \sim D_0 t$. Here, D_0 is a known function of the particle density and the external bias [2], and is given later in the paper.

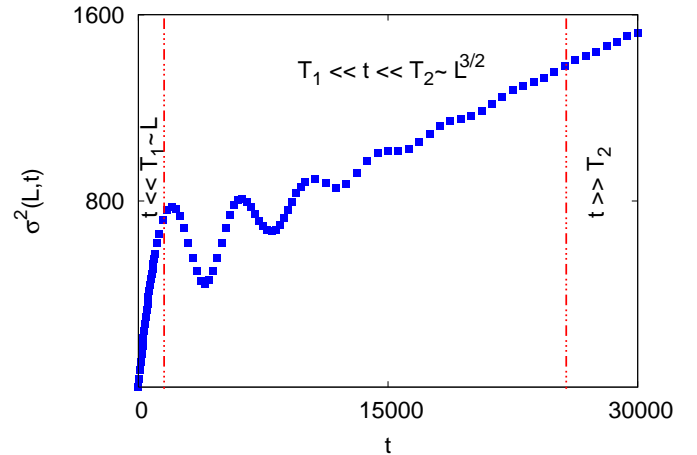


FIG. 1: (Color online) Monte Carlo (MC) simulation results for the time dependence of the variance $\sigma^2(L, t)$ for the TASEP on a finite lattice, averaged over 10^5 MC runs. The different time regimes are also marked. Here, $L = 1024$, the particle density $\rho = 0.25$.

(b) In the opposite limit with $t \rightarrow \infty$ before $L \rightarrow \infty$, $\sigma^2(L, t)$ again behaves diffusively, i.e., $\sigma^2(L, t) \sim D(L)t$, but now the diffusion constant $D(L)$ depends on the sys-

tem size L and scales as $D(L) \sim \frac{1}{\sqrt{L}}$ for large L [3]. A natural question arises: What is the full behavior of $\sigma^2(L, t)$ as a function of time in between these two extremes? In this paper, we show that in the intermediate regime, $\sigma^2(L, t)$ shows striking oscillations as a function of time. Indeed, there are two time-scales in the problem, $T_1 \sim L$ and $T_2 \sim L^{3/2}$. The limiting behaviors (a) and (b) hold in the regimes $t \ll T_1$ and $t \gg T_2$, respectively, and in between ($T_1 \ll t \ll T_2$), the quantity $\sigma^2(L, t)$ oscillates with time, as shown in Fig. 1.

In measuring the fluctuations, if one does not start from the stationary ensemble, but instead from an arbitrary but *fixed* configuration drawn from the stationary ensemble, the corresponding variance $s^2(L, t)$ of the displacement behaves very differently from $\sigma^2(L, t)$. The behavior of $s^2(L, t)$, in the limit of an infinite system, is known: $s^2(t) \equiv \lim_{L \rightarrow \infty} s^2(L, t) \sim t^{2/3}$ [4]. For a finite system, we find a similar growth until a characteristic time $T^* \sim L^{3/2}$, after which this correlation grows linearly in time: $s^2(L, t) \sim D(L)t$ with $D(L) \sim \frac{1}{\sqrt{L}}$.

Some of the results for the tagged particle correlations discussed in this paper were known previously. However, a complete and a consistent picture on a finite lattice is lacking in the literature. The principal purpose of this paper is to discuss finite size effects on the tagged particle correlation in the ASEP on a one-dimensional ring from a unified point of view. In order to do this, we include some known results for completeness, in addition to the new results on the finite size effects. The main results are summarized below.

1. The behavior of $\sigma^2(L, t)$ as a function of time can be characterized by two time scales $T_1 \sim L$ and $T_2 \sim L^{3/2}$, as shown in Fig. 1.

(a) In the initial linear regime ($t \ll T_1$), the variance $\sigma^2(L, t) \sim D_0 t$ [7].

(b) In the oscillatory regime ($T_1 \ll t \ll T_2$), the quantity $\sigma^2(L, t)$ oscillates as a function of t . The amplitude of oscillations is proportional to the system size L while the time period of oscillations is $T = L/u$, where u is the mean velocity of the stationary state density fluctuations relative to the average drift velocity of the particles.

(c) In the late time regime ($t \gg T_2$), the quantity $\sigma^2(L, t) \sim D(L)t$ with $D(L) \sim \frac{1}{\sqrt{L}}$.

2. The time variation of $s^2(L, t)$ can be characterized by a single time scale $T^* \sim L^{3/2}$. The variation of $s^2(L, t)$ with time for two different system sizes is shown in Fig. 2.

(a) $t \ll T^*$: In this regime, $s^2(L, t) \sim t^{2/3}$.

(b) $t \gg T^*$. Here, $s^2(L, t) \sim D(L)t$ with $D(L) \sim \frac{1}{\sqrt{L}}$.

The long-time behavior of both the functions $\sigma^2(L, t)$ and $s^2(L, t)$ is diffusive, with the same diffusion constant $D(L)$ which scales with the system size as $D(L) \sim \frac{1}{\sqrt{L}}$. This behavior is attributed to the motion of the center-of-mass.

The physical origin of oscillations in $\sigma^2(L, t)$ is the occurrence of kinematic waves that transport stationary state density fluctuations through the system (Appendix

A). Kinematic waves are known to arise in a variety of circumstances involving flow e.g., in flood movement in long rivers [8], traffic [9, 10], flow of granular particles through vertical tubes and hoppers [11], motion of transverse fluctuations in interfaces [12, 13], field-induced transport in random media as in drop-push dynamics [14]. In our system, the velocity of the sliding density fluctuations (SDF) relative to the average drift of the ASEP particle determines the period of the oscillations. Eventually, the oscillations damp down as the density fluctuations dissipate owing to the stochasticity and non-linearity inherent in the dynamics. This dissipation in time is well captured by the temporal behavior of the function $s^2(L, t)$, as we show in this paper.

3. The ASEP can be mapped to a non-equilibrium model of interface growth in the Kardar-Parisi-Zhang (KPZ) universality class [15]. The resultant time evolution equation for the interface is the usual KPZ equation, augmented by a drift term which accounts for the SDF. In this paper, we consider the interface equation with the drift term in the linear approximation, and solve exactly for $\sigma^2(L, t)$ and $s^2(L, t)$. Our analytical solution of the linearized model captures the essential qualitative features seen in these two quantities for the ASEP. Moreover, we show that the linearized model is an exact coarse-grained description of two specific microscopic models of interacting particles, the Katz-Lebowitz-Spohn (KLS) model [16] at a specific value of the temperature and the Asymmetric Random Average Process (ARAP) [17]. Our analytic solution quantitatively describes the behavior of the tagged particle correlations for these two models.

The paper is organized as follows. In Section II, we define the model and the variances $\sigma^2(L, t)$ and $s^2(L, t)$ of the tagged particle process, followed by a discussion in the context of the KPZ interface equivalent to the ASEP. In Section III, we give a representation for the tagged particle displacement on an infinite lattice, and show how it correctly accounts for the known results for the variance. This is followed by Section IV where we adduce physical arguments for the observed behavior of $\sigma^2(L, t)$ and $s^2(L, t)$, both on an infinite as well as a finite lattice. The time-evolution equation for the interface-equivalent of the ASEP is solved exactly in the linear approximation in Section V which explains some qualitative features of the tagged particle correlations for the ASEP. As we show in Section VI, the exact solution also explains quantitatively the variance of the tagged particle displacement for the KLS model at a specific value of the temperature and for the ARAP. In Section VII, we discuss the center-of-mass motion for the ASEP, followed by conclusions in Section VIII.

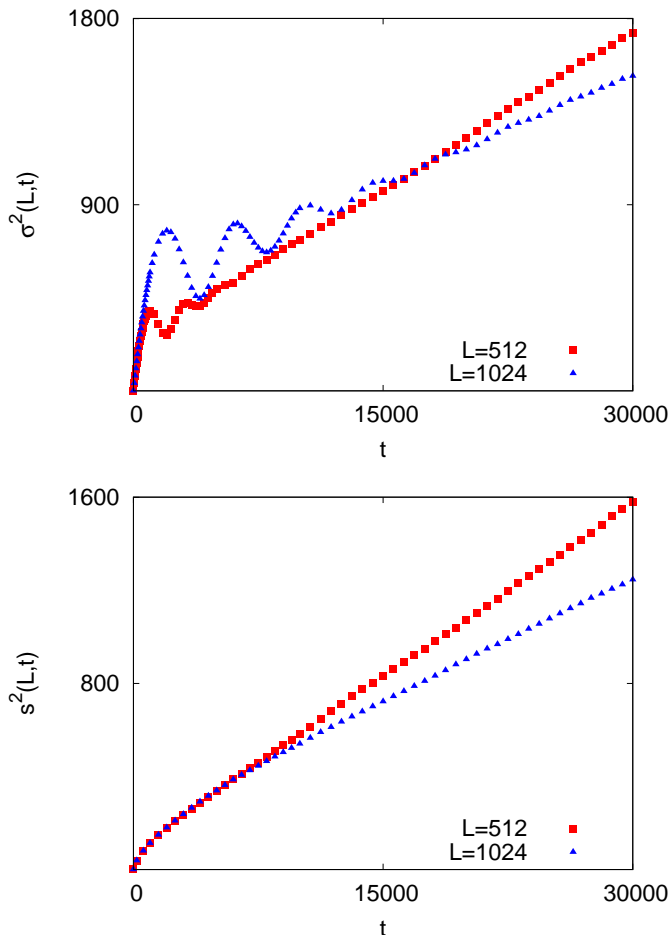


FIG. 2: (Color online) MC simulation results for the time dependence of the variance of the displacement for the TASEP on a finite lattice for $\sigma^2(L, t)$ and $s^2(L, t)$. In both cases, the averaging is over 10^5 MC runs. Here, the density $\rho = 0.25$. The two system sizes are 512 and 1024.

II. TAGGED PARTICLE CORRELATIONS

A. The Model

We consider the ASEP on a periodic lattice of L sites. N indistinguishable hard core particles are distributed over the lattice sites with each site either singly-occupied or empty. The particle density $\rho = \frac{N}{L}$ is held constant when the limit $L \rightarrow \infty, N \rightarrow \infty$ is taken. Let $n_i = 0, 1$ with $i = 1, 2, \dots, L$ denote the occupancy of the i -th site. The system evolves according to a stochastic dynamics: during an infinitesimal time interval dt , a particle attempts to hop to the site to its right with probability pdt , to the left neighboring site with probability qdt , and continues to occupy the original site with probability $1 - (p+q)dt$. The attempted hop is successful only if the sought site is empty before the hop. L attempted hops constitute one time step. Clearly the total number of par-

ticles is conserved under the dynamics. For the TASEP, the motion of the particles is entirely in one direction i.e., $p = 1$ and $q = 0$ or, vice-versa. Note that with $p = q$, each particle moves symmetrically to the left and to the right. The model then reduces to the symmetric Simple Exclusion Process (SEP), an equilibrium model of hard core particles diffusing on a lattice.

It is evident from the rule of evolution that the dynamics is ergodic. In the limit $t \rightarrow \infty$, the system settles into a nonequilibrium stationary state. Ergodicity ensures uniqueness of the stationary state. On a lattice of size L , the stationary state is one in which all configurations \mathbf{C} have the same weight $p(\mathbf{C}) = \frac{N!(L-N)!}{L!}$ [1]. It then follows that the two-point correlation function in the stationary state $\overline{n_i n_j} = \frac{N(N-1)}{L(L-1)}$ for $i \neq j$. Here, as in the rest of the paper, the overbar is used to denote an average over the stationary ensemble of configurations. In the thermodynamic limit, the steady state has a product measure form. In the stationary state, the ASEP supports a steady current of particles whose mean value $J = (p - q)\overline{n_i(1 - n_{i+1})}$ for a system of size L is given by $J = (p - q)\rho(1 - \rho) + O(\frac{1}{L})$. Correspondingly, the mean velocity of a particle in the stationary state, given by $v_P = \frac{J}{\rho}$, equals $v_P = (p - q)(1 - \rho) + O(\frac{1}{L})$.

Besides particle motion, there is also a motion associated with the coarse-grained density fluctuations in the stationary state of the ASEP. The density fluctuations are transported as a kinematic wave with velocity $v_K = \frac{\partial J}{\partial \rho}$ (see Appendix A). Thus, relative to the average drift of the particles, the density fluctuations ‘slide’ with velocity $v_K - v_P$. We refer to this relative motion as the sliding density fluctuations (SDF). Stochasticity and nonlinearity in the dynamics lead to dissipation of the density profile so that the wave of fluctuations ultimately dies down in time. The kinematic wave velocity for an infinite system is given by $v_K = (p - q)(1 - 2\rho)$. This velocity, derived on the basis of hydrodynamic considerations discussed in Appendix A, also appears as the imaginary part of the low-lying eigenvalues of the Markov matrix governing the time evolution of the ASEP in the totally asymmetric case $q = 0$ [18]. Figure 3 shows the time evolution of a stationary ASEP configuration. One clearly sees that the space-time trajectory of a particle is distinctly different from that for a coarse-grained density fluctuation.

B. Two different observables

The primary quantity of interest in this paper is the variance of the displacement of a tagged particle around its mean trajectory. Note that the displacement $y(n, t)$ of the n -th particle in time t ranges from $-\infty$ to ∞ even though the system size L is finite.

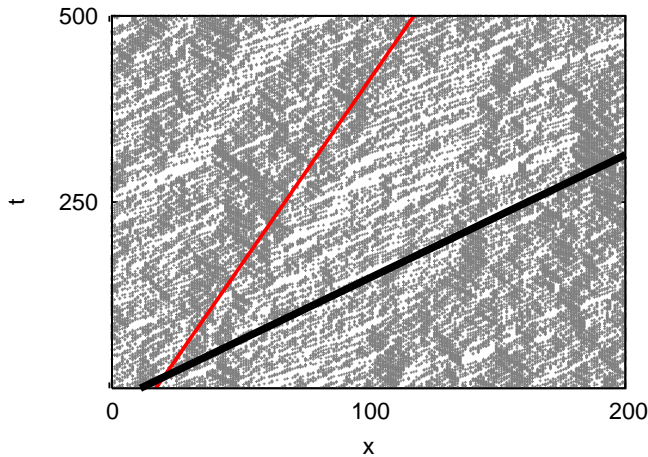


FIG. 3: (Color online) Time evolution for a stationary TASEP configuration. Here, the system size $L = 200$, the density $\rho = 0.4$. The inverse of the slope of the thick black line is the velocity of the tagged particle $v_P \approx (p - q)(1 - \rho) = 0.6$ while that of the thin red line is the velocity of the density fluctuations $v_K \approx (p - q)(1 - 2\rho) = 0.2$.

1. Average over histories and initial conditions: $\sigma^2(L, t)$

Here we start with the stationary ensemble of the ASEP configurations at $t = 0$ and monitor the motion of a tagged particle. Let $\Delta_n(t)$ denote the deviation in the displacement of the n -th tagged particle from its average value in time t , the averaging being with respect to both the initial stationary ensemble at $t = 0$ and stochasticity in the evolution of configurations. In symbols,

$$\Delta_n(t) \equiv y(n, t) - y(n, 0) - \overline{\langle [y(n, t) - y(n, 0)] \rangle} \quad \text{[Ensemble of Initial Conditions]}. \quad (1)$$

The angular brackets denote averaging over the stochasticity in the evolution of configurations, while the overbar is used to denote averaging with respect to the initial stationary ensemble at $t = 0$. In the function $\Delta_n(t)$, the quantity $\overline{\langle [y(n, t) - y(n, 0)] \rangle}$ gives the average displacement of the n -th tagged particle in time t in the stationary state, and hence is equal to $v_P t$. The variance of the displacement, measuring the stationary state fluctuations

in $\Delta_n(t)$, is given by

$$\sigma^2(L, t) \equiv \overline{\langle \Delta_n^2(t) \rangle}. \quad (2)$$

Since the system is translationally invariant, the above quantity is the same for all particles, and hence we do an additional averaging of $\sigma^2(L, t)$ over the particles.

In this paper, we study how the finiteness of the system size L affects the behavior of $\sigma^2(L, t)$ in time.

2. Average over histories only: $s^2(L, t)$

Beginning with an arbitrary but *fixed* configuration, chosen from the stationary ensemble and following its evolution in time, it is interesting to monitor the fluctuations in the displacement of a tagged particle, and study how finite size effects come into play here. These fluctuations were first studied by van Beijeren for an infinite system in [4]. In this case, one averages only over the stochasticity in the evolution of the configuration. We define $d_n(t)$ to be the deviation in the displacement of the n -th tagged particle from its mean value in time t , starting from an arbitrary but fixed configuration, drawn from the stationary ensemble at $t = 0$. Explicitly,

$$d_n(t) \equiv y(n, t) - y(n, 0) - \langle [y(n, t) - y(n, 0)] \rangle \quad \text{[Fixed Initial Condition]}. \quad (3)$$

The corresponding variance is given by

$$s^2(L, t) \equiv \langle d_n^2(t) \rangle. \quad (4)$$

The system being translationally invariant, the above quantity is also averaged over the particles.

We note that the behavior of both $\sigma^2(L, t)$ and $s^2(L, t)$ can be extracted from two different limiting values of a single function that measures the fluctuation in the displacement of a tagged particle in the stationary state. At time $t = 0$, we start with an arbitrary but fixed configuration \mathbf{C}_0 , drawn from the stationary ensemble of configurations. After \mathbf{C}_0 has evolved in time for an interval t_0 , we start measuring the variance $C_L(t_0, t_0 + t)$ of the displacement of a tagged particle around its average:

$$C_L(t_0, t_0 + t) \equiv \langle [y(n, t_0 + t) - y(n, t_0) - \langle [y(n, t_0 + t) - y(n, t_0)] \rangle]^2 \rangle, \quad (5)$$

where the angular brackets denote averaging with respect to stochastic evolution.

(1) On taking the limit $t_0 \rightarrow 0$, when the averaging is only with respect to stochastic evolution, we get the function $s^2(L, t)$.

(2) On the other hand, since the system is ergodic, in the limit $t_0 \rightarrow \infty$, the initial configuration \mathbf{C}_0 evolves into an ensemble of stationary configurations. Thus, the function $\lim_{t_0 \rightarrow \infty} C_L(t_0, t_0 + t)$ measures fluctuations in the stationary state where the averaging is with respect

to both the initial stationary ensemble and stochastic evolution. Hence, this quantity is identical to $\sigma^2(L, t)$.

C. Interface equivalent

Many of our results for $\sigma^2(L, t)$ and $s^2(L, t)$ can be explained in terms of the continuum description of the ASEP, achieved by mapping it to a model of nonequilibrium interface growth [5] that belongs to the KPZ universality class of nonequilibrium interface dynamics [15]. The mapping that we use in this paper employs the tagging process of the particles in a direct and essential way in the translation [19]. Let the particles be labeled $1, 2, \dots, N$ sequentially at the initial instant. Since the particle motion is in one dimension, and there is no overtaking, this labeling will be preserved for all subsequent times. The corresponding interface is obtained by identifying the tag label n with the horizontal coordinate n for the interface, while the set $\{y(n, t)\}$, denoting the particle locations at time t , maps onto the set of local interface heights $\{h(n, t)\}$ defined by

$$h(n, t) = y(n, t) - \frac{n}{\rho}. \quad (6)$$

Since the inequality $y(n+1, t) \geq y(n, t) + 1$ holds, it follows that the interface heights satisfy $h(n+1, t) \geq h(n, t) + 1 - \frac{1}{\rho}$. Periodic boundary condition implies $y(n \pm N) = y(n) \pm L$, and correspondingly, $h(n \pm N, t) = h(n, t)$.

The dynamics of the interface involves the following moves in a small time interval dt : the move $h(n, t) \rightarrow h(n, t + dt) = h(n, t) + 1$ occurs with probability pdt while the move $h(n, t) \rightarrow h(n, t + dt) = h(n, t) - 1$ takes place with probability qdt . The interface height remains the same with probability $1 - (p+q)dt$. The attempt to increase, respectively decrease, succeeds only if $y(n+1, t) - y(n, t) > 1$, respectively $y(n, t) - y(n-1, t) > 1$.

ASEP	Lattice Interface Model
Particle Label n	Spatial coordinate n
Displacement $y(n, t)$	Height $h(n, t) + \frac{n}{\rho}$
Mean Velocity v_P	Mean growth rate $\frac{\partial \langle h \rangle}{\partial t}$

TABLE I: Mapping ASEP to the interface.

Following the above prescription, the ASEP with N particles and L sites maps onto a lattice model of the interface of length N . In order to get the continuum equation for the interface, we (i) coarse-grain the particle labels so that the discrete tag label n becomes the continuous tag variable x , and (ii) divide x by the particle density ρ to make x into a spatial variable running between 0 and L . The equation of motion of the interface, to lowest order of nonlinearity, is given by

$$\frac{\partial h(x, t)}{\partial t} = v_P + \Gamma \frac{\partial^2 h}{\partial x^2} + u \frac{\partial h}{\partial x} + \frac{\lambda}{2} \left(\frac{\partial h}{\partial x} \right)^2 + \eta(x, t), \quad (7)$$

where $v_P = (p - q)(1 - \rho)$, $\Gamma = \frac{1}{2}$, $u = \rho(p - q)$, $\lambda = -2\rho(p - q)$. Here, $\eta(x, t)$ represents a Gaussian noise with $\langle \eta(x, t) \rangle = 0$, $\langle \eta(x, t) \eta(x', t') \rangle = 2A\delta(x - x')\delta(t - t')$, where $A = \frac{1}{2} \left(\frac{1 - \rho}{\rho} \right)$. The boundary condition $h(n \pm N, t) = h(n, t)$ on the height variable for the discrete interface now reads $h(x \pm L, t) = h(x, t)$ in the continuum. The derivation of Eq. 7 is relegated to the Appendix B. The constant term v_P and the drift term $u \frac{\partial h}{\partial x}$ in Eq. 7 can be eliminated by a boost and a Galilean shift, respectively, as explained below. In that case, Eq. 7 describes the time evolution equation of a KPZ interface [15]. Note that Eq. 7 is not an exact description of the time evolution for the ASEP density profile. It is rather a coarse-grained description of the ASEP. One expects that the scaling properties of the correlation functions for both the ASEP and its interface-equivalent are governed by the same KPZ fixed point, and hence, are described by the same critical exponents and scaling functions.

For the symmetric exclusion process (SEP), the corresponding interface is an equilibrium one that does not move bodily. Rather, it fluctuates about a stationary profile, and its time evolution is governed by the Edwards-Wilkinson (EW) equation [20], obtained by setting $p = q$, implying $v_P = 0$, $u = 0$, $\lambda = 0$, so that

$$\frac{\partial h(x, t)}{\partial t} = \Gamma \frac{\partial^2 h}{\partial x^2} + \eta(x, t). \quad (8)$$

On including all the higher order nonlinearities, Eq. 7 is replaced by the general form

$$\frac{\partial h(x, t)}{\partial t} = \Gamma \frac{\partial^2 h}{\partial x^2} + \sum_{m=0}^{\infty} \lambda_m \left(\frac{\partial h}{\partial x} \right)^m + \eta(x, t), \quad (9)$$

where, e.g., $\lambda_0 = v_P$, $\lambda_1 = u$, $\lambda_2 = \lambda/2$, etc. The different coefficients λ_m in Eq. 9 determine the scaling properties of the height fluctuations, as discussed below. λ_0 can be eliminated by redefining the height variable $h \rightarrow h' = h + \lambda_0 t$. The first-order gradient term, $\lambda_1 \frac{\partial h}{\partial x}$, can be eliminated from Eq. 9 by Galilean shift $x \rightarrow x' = x + \lambda_1 t$.

The stationary state height fluctuations are measured by

$$S(x, t) = \overline{\langle [h(x + x', t) - h(x', 0)]^2 \rangle} - \left[\overline{\langle h(x + x', t) - h(x', 0) \rangle} \right]^2, \quad (10)$$

where the angular brackets denote averaging over the stochastic evolution of the interface, while the overbar represents averaging over the initial stationary ensemble of the interface configurations.

If λ_1 is nonzero, the autocorrelation function grows as $S(0, t) \sim t$ for large t [5, 6, 12]. This can be explained in terms of sliding density fluctuations (SDF) with respect to the particle motion, as discussed in Section IV. If $\lambda_0 = \lambda_1 = 0$, the function $S(x, t)$ assumes the scaling form

$$S(x, t) \sim t^{2\beta} Y \left(\frac{x}{t^{1/z}} \right) \quad (11)$$

in the asymptotic limit $x, t \rightarrow \infty$, with $x/t^{1/z} = \text{constant}$. Here, β is the growth exponent while z is the dynamical exponent. These exponents as well as the scaling function Y are the same for all systems belonging to the same universality class. The scaling function $Y(s)$ has the property that $Y(s) \rightarrow \text{constant}$ as $s \rightarrow 0$, implying that the height autocorrelation $S(0, t) \sim t^{2\beta}$. Further, as $s \rightarrow \infty$, the function $Y(s) \rightarrow s^{2\alpha}$. Here, α is the critical exponent related to z and β through $z = \alpha/\beta$ [21]. It determines the roughness of the interface, $S(x, 0) \sim x^{2\alpha}$.

From a perturbative renormalization group (RG) analysis of Eq. 9, it is known that there are two distinct fixed points in the parameter space. These two fixed points define two universality classes. The first class is the one in which all $\lambda_m = 0$. In this case, Eq. 9 reduces to the EW equation, Eq. 8. The resulting linear growth problem was also studied by Hammersley in a different context [22]. The values of the critical exponents for this class are [20]

$$\beta = 1/4, z = 2 \quad (\text{EW in 1d}). \quad (12)$$

The Edwards-Wilkinson (EW) fixed point also controls the behavior in systems where only odd-order terms λ_m with $m \geq 3$ are present. The lowest-order nonlinearity is provided by the cubic term. Under a scaling transformation $x \rightarrow x' = bx, t \rightarrow t' = b^z t, h \rightarrow h' = b^\alpha h$, we see that the cubic nonlinear term is marginal around the EW fixed point. Calculations based on mode coupling theory [23] and RG [24, 25] show that it is actually marginally irrelevant, leading to multiplicative logarithmic corrections to the power law: $S(0, t) \sim t^{1/2}(\ln t)^{1/4}$, a behavior that has been verified by numerical simulation study [24, 25, 26].

Even-order coefficients lead to a breaking of $h \rightarrow -h$ symmetry of Eq. 9, causing a change in the universality class. The second-order perturbation λ_2 is a relevant perturbation for the EW fixed point that drives the system away from the EW to a new KPZ fixed point. The KPZ fixed point is characterized by the exponent values [15]

$$\beta = 1/3, z = 3/2 \quad (\text{KPZ in 1d}). \quad (13)$$

If $\lambda_1 \neq 0$, under the scaling transformation $x \rightarrow x' = bx, t \rightarrow t' = b^z t, h \rightarrow h' = b^\alpha h$, both the EW and KPZ fixed points are unstable, and a flow towards a third fixed point (SDF) is generated (Fig. 4), as we show in this paper.

III. REPRESENTATION FOR AN INFINITE SYSTEM

On the basis of the discussion in Section II, we conclude that in the stationary state, the displacement of the n -th tagged particle, $y(n, t) - y(n, 0)$, has contributions from three distinct physical sources, namely, systematic

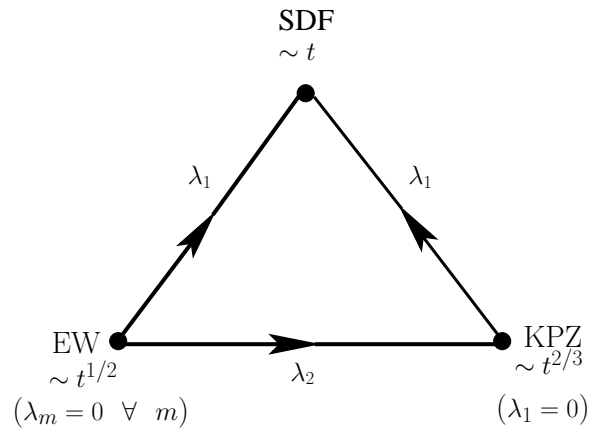


FIG. 4: Schematic representation of relative stabilities of various fixed points, showing the associated behavior of the variance $\sigma^2(L, t)$ of the displacement of the tagged particle in an infinite system.

drift, sliding density fluctuations, and their dissipation. Correspondingly we write

$$y(n, t) - y(n, 0) \approx v_P t + t^\alpha G_n(t) + t^\beta \chi_n(t), \quad (14)$$

where $\alpha = \alpha_{KPZ} = 1/2$ is the roughness exponent while $\beta = \beta_{KPZ} = 1/3$ is the growth exponent of the interface equivalent to the ASEP. The representation, Eq. 14, is based on the following arguments. First, the coarse-grained density fluctuations for the ASEP are described by the KPZ interface whose fluctuation profile moves with velocity $v_K - v_P$. As a result, in time t , the particle senses the fluctuations over a stretch of length $(v_K - v_P)t$. From the scaling analysis of the interface summarized in Section II, the typical fluctuation over this distance scales as $[(v_K - v_P)t]^\alpha \sim t^\alpha$. This fact is encoded in the second term in Eq. 14 where $G_n(t)$ is a random variable which depends only on the initial configuration, drawn from the stationary ensemble, but is independent of the stochastic noise in the evolution of configurations. The fluctuations arising from the dissipation typically grow with time as t^β and are represented by the last term in Eq. 14. Here $\chi_n(t)$ is a random variable that depends only on the noisy history in the evolution of configurations, but is independent of the initial configuration.

We show below how the form, Eq. 14, accounts for the observed behavior of correlation functions for an infinite system.

- On averaging with respect to both the initial stationary ensemble and stochastic evolution, we get

$$\overline{\langle y(n, t) - y(n, 0) \rangle} \approx v_P t + t^\alpha \overline{G_n} + t^\beta \langle \chi_n \rangle, \quad (15)$$

where, as previously, the angular brackets denote averaging with respect to the stochastic evolution, while the overbar is used to denote averaging with respect to the initial stationary ensemble.

It follows that for the variable defined in Eq. 1,

$$\Delta_n(t) \approx t^\alpha(G_n - \overline{G_n}) + t^\beta(\chi_n - \langle\chi_n\rangle). \quad (16)$$

With $\alpha = 1/2$ and $\beta = 1/3$ for the ASEP, the first term on the rhs dominates for large t . We recover the result for $\sigma^2(L, t) = \overline{\langle\Delta_n^2(t)\rangle}$ for an infinite system [2] (described in the Introduction), given by

$$\lim_{L \rightarrow \infty} \sigma^2(L, t) \stackrel{t \rightarrow \infty}{\sim} \overline{t(G_n - \overline{G_n})^2} \sim t. \quad (17)$$

- For fixed initial condition, averaging over noise history, we get

$$\langle y(n, t) - y(n, 0) \rangle \approx v_P t + t^\alpha G_n + t^\beta \langle \chi_n \rangle. \quad (18)$$

Thus, for the displacement variable defined in Eq. 3, we have

$$d_n(t) \approx t^\beta [\chi_n - \langle \chi_n \rangle]. \quad (19)$$

The fluctuations in $d_n(t)$ are measured by $s^2(L, t)$ according to the definition, Eq. 4. Thus, one has

$$s^2(t) = \lim_{L \rightarrow \infty} s^2(L, t) \stackrel{t \rightarrow \infty}{\sim} t^{2\beta} \langle (\chi_n - \langle \chi_n \rangle)^2 \rangle \sim t^{2\beta}. \quad (20)$$

With $\beta = 1/3$, we get the result $s^2(t) \sim t^{2/3}$ [4] for the growth of the variance of the displacement of a tagged particle in an infinite system, starting from an arbitrary fixed initial configuration drawn from the stationary ensemble, as discussed in the Introduction.

IV. VARIANCES $\sigma^2(L, t)$ AND $s^2(L, t)$: PHYSICAL ARGUMENTS

A. Infinite system

The variance $\sigma^2(t)$ of the displacement of a tagged particle in an infinite system, averaged with respect to both the initial stationary ensemble and stochastic evolution, behaves very differently from the variance $s^2(t)$ where the averaging is with respect to only the stochastic evolution. Such differences for an infinite system have also been observed for shock fluctuations in the ASEP [27]. In this subsection, we provide physical interpretations of the observed linear growth in time for $\sigma^2(t)$ and the $t^{2/3}$ growth of $s^2(t)$.

1. $\sigma^2(t)$

As the averaging in Eq. 2 is with respect to both an initial stationary ensemble and stochastic noise in the evolution of configurations, the average drift in time t is $v_P t$, and fluctuations in the tagged particle displacement are defined with respect to this. In the rest frame of the

density fluctuations, the tagged particle has an average velocity $u = v_P - v_K$. In time t , it traverses a sequence of density fluctuations over a distance $(v_P - v_K)t$, with each fluctuation adding a stochastic noise to the motion of the tagged particle. The noise is uncorrelated since the stationary state configurations have a product measure. The variance $\sigma^2(L, t)$ is thus proportional to t for large t , by virtue of the central limit theorem. The coefficient of proportionality D_0 is known to be $v_P = (p - q)(1 - \rho)$ [2]. This expression for D_0 can be easily derived using the above picture of drift of the tagged particles relative to the density fluctuations [12].

2. $s^2(t)$

For $s^2(t)$, the fluctuations are measured by starting from a single fixed configuration, drawn from the ensemble of stationary states. Thus, in every measurement, the particle passes through the *same* sequence of density fluctuations. However, dissipation of the density profile is different from history to history.

Define the deviation in the displacement of a tagged particle from $v_P t$ by

$$D_n(t) = y(n, t) - y(n, 0) - v_P t. \quad (21)$$

The dissipation in the density profile being different for different histories shows up in $D_n(t)$, as depicted by the gray trajectories in Fig. 5. Notice that the mean over histories, $\langle D_n(t) \rangle$, is nonvanishing, as depicted by the black curve in Fig. 5.

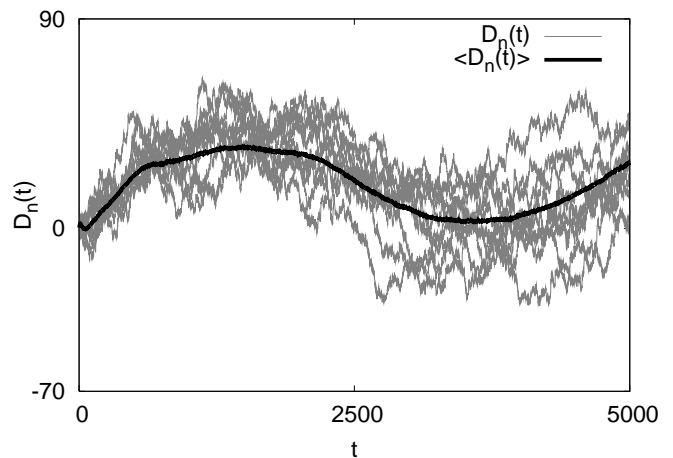


FIG. 5: The gray curves show the distance covered, $D_n(t)$, in time t about the mean $v_P t$ by the n -th tagged particle for 10 Monte Carlo runs for a single fixed initial configuration, drawn from the stationary ensemble of the TASEP. The black curve shows the mean displacement, $\langle D_n(t) \rangle$, obtained by averaging over 500 histories. Here, $L = 10,000$, the particle density $\rho = 0.25$.

Since the variance $s^2(t)$ of the fluctuation in Eq. 4 is measured with respect to $v_P t + \langle D_n(t) \rangle$, it is able to sense

the dissipation of the density profile in time, without the effects of SDF. From Eq. 14, with $\alpha = 1/2$ and $\beta = 1/3$, we get $D_n(t) = t^{1/2}G_n(t) + t^{1/3}\chi_n(t)$; on averaging over stochastic evolution, we get

$$\langle D_n(t) \rangle = t^{1/2}G_n(t) + t^{1/3}\langle \chi_n(t) \rangle. \quad (22)$$

The first term in Eq. 22 dominates, and thus at large t , $\langle D_n(t) \rangle$ is primarily determined by the pattern of spatial density fluctuations in the initial configuration. Ignoring the dissipative component (the second term in Eq. 22), we expect $\langle D_n(t) \rangle$ to be given by $D_n^*(t) \approx (p - q) \int_0^t dt' \{(1 - \rho(x)) - (1 - \rho)\}$. Making a change of variable from t to x , and noting that the Jacobian of transformation is $1/(v_P - v_K)$, we get

$$D_n^*(t) \approx \frac{(p - q)}{v_P - v_K} \int_{y(n,0)}^{y(n,0) + (v_P - v_K)t} dx \{(1 - \rho(x)) - (1 - \rho)\}. \quad (23)$$

The upper limit of the integral incorporates the relative distance moved by the particle, $(v_P - v_K)t$, neglecting fluctuations of $O(t^{1/2})$ coming from the second term in Eq. 14.

In Fig. 6, we have compared $\langle D_n(t) \rangle$ with $D_n^*(t)$ for a randomly chosen initial configuration. $\langle D_n(t) \rangle$ was obtained from simulations, while $D_n^*(t)$ was obtained by integrating the initial density profile, following Eq. 23. We see that there is good agreement between the signals for $\langle D_n(t) \rangle$ and $D_n^*(t)$. Fluctuations over a distance δx dissipate in a time $t \sim (\delta x)^z$ with $z = 3/2$. Thus, with increasing t , spatial fluctuations in the initial profile are smeared out over larger distances, a fact which is borne out by Fig. 6. We have also measured the overlap function for the signs of the two signals, $\langle D_n(t) \rangle$ and $D_n^*(t)$, for 10 different randomly chosen initial configurations at stationarity, and found a mean value 0.8, which indicates a fairly good degree of correlation between the two signals.

B. Finite system

We now turn to the behavior of $\sigma^2(L, t)$ and $s^2(L, t)$ on a finite lattice, and explain the differences in their behavior on the basis of SDF.

1. $\sigma^2(L, t)$

In the rest frame of the density fluctuations, a tagged particle has velocity $u = v_P - v_K$ and would take time $T = L/u$ to return to its initial environment of density fluctuations. Thus the variance of the tagged particle displacement should increase from 0 at $t = 0$, reach a maximum at around $T/2$, and come down to almost zero at $t = T$. The difference from zero at $t = T$ is due to dissipation in the density profile arising from stochasticity in the dynamics. This scenario recurs at integral T 's; the time period of oscillations is $T = L/u = L/[(p - q)\rho]$

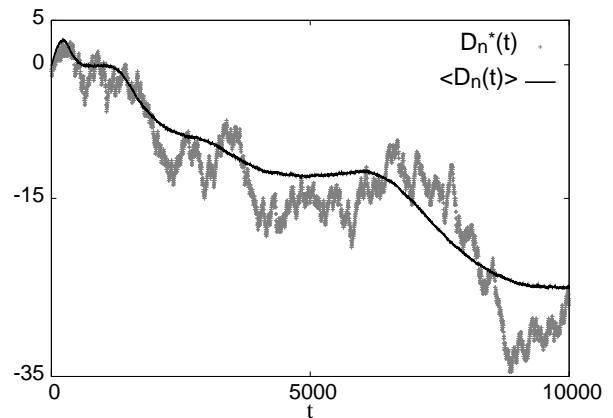


FIG. 6: Comparison between $\langle D_n(t) \rangle$ and $D_n^*(t)$ for a fixed initial stationary configuration of the TASEP. $\langle D_n(t) \rangle$ was obtained from simulations, and involves averaging over 1000 histories. $D_n^*(t)$ was obtained by integrating the initial density profile according to Eq. 23 (see text). Here, $L = 10,000$, while the density $\rho = 0.25$.

The oscillations do not continue forever because of the cumulative effect of dissipation. An estimate for the time taken to completely dissipate an initial pattern of density fluctuations is $T_2 \sim L^z$, where the dynamical exponent z is known to have the value $3/2$ [28]. For times $t \gg T_2$, when the initial density profile has completely dissipated away, the fluctuations are entirely due to the motion of the center-of-mass: $\sigma^2(L, t) \sim D(L)t$ with $D(L) \sim \frac{1}{\sqrt{L}}$. The scaling of $D(L)$ with the system size L is obtained by matching the behavior of $\sigma^2(L, t)$ across T_2 .

The lower envelope $\Lambda^2(L, t)$ of the oscillations in $\sigma^2(L, t)$ is determined by the dissipation of the stationary state density profile, and can be studied by the method of sliding tags [5, 6, 12, 24, 25, 29, 30, 31]. In order to monitor the dissipation of the moving density profile, we need to correlate, at different times, the location of two different particles. Since in the frame of the density fluctuations, particles move with velocity $u = v_P - v_K$, we need to examine the function

$$\Lambda^2(L, t) = \overline{\langle [y(n', t) - y(n, 0)]^2 \rangle} - \overline{\langle [y(n', t) - y(n, 0)] \rangle}^2, \quad (24)$$

where

$$n' = n - \rho ut. \quad (25)$$

The tag shift ρut accounts for the relative motion of the particles and the density profile, and ensures that the time evolution of the same density patch is being recorded at every instant. Equation 25, representing sliding of the tag, is tantamount to a Galilean shift that gets rid of the drift term, $u \frac{\partial h}{\partial x}$, in Eq. 7. In Fig 7, we show how the method of sliding tags discussed above gives the lower envelope $\Lambda^2(L, t)$ of the oscillatory quantity $\sigma^2(L, t)$. This envelope grows with time as $t^{2/3}$ until times $\sim L^{3/2}$, beyond which $\Lambda^2(L, t) \sim D(L)t$ with

$D(L) \sim \frac{1}{\sqrt{L}}$. Thus, beyond $T_2 \sim L^{3/2}$, there is no distinction between the temporal behavior of $\sigma^2(L, t)$ and $\Lambda^2(L, t)$.

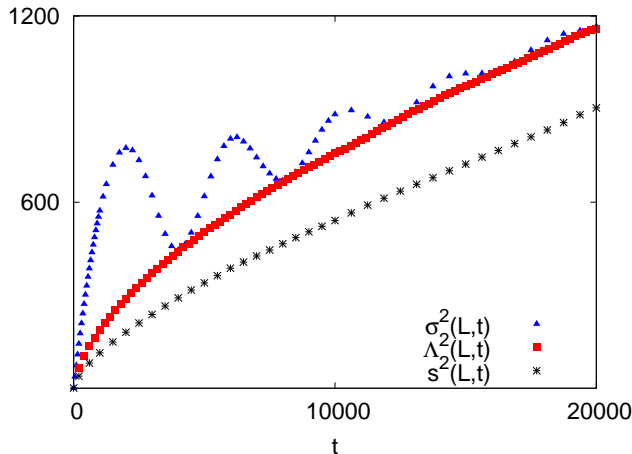


FIG. 7: (Color online) MC simulation results for various tagged particle correlations. The topmost curve refers to the variance $\sigma^2(L, t)$ of the displacement when the averaging is over both the initial stationary ensemble and stochastic evolution. The middle curve is the sliding tag correlation function $\Lambda^2(L, t)$ defined in the text; it coincides with $\sigma^2(L, t)$ at the local minima of the latter. The lowermost curve shows the variance $s^2(L, t)$ when the averaging is only over stochastic evolution. Here, $\rho = 0.25$. The system size is 1024. The averaging is over 10^5 MC runs.

2. $s^2(L, t)$

Since we always use the same initial condition in this case, the particle moves through the same sequence of

density fluctuations in every measurement. Nevertheless, the dissipation of the density profile is different for different histories, and $s^2(L, t)$ captures this. Typical fluctuation grows with time as $t^{1/3}$, following Eq. 14. This leads to $s^2(L, t) \sim t^{2/3}$. This behavior continues until $t \gg T^* \sim L^{3/2}$ when the fluctuations are due to the diffusive motion of the center-of-mass. This gives $s^2(L, t) \sim D(L)t$ with $D(L) \sim \frac{1}{\sqrt{L}}$. One obtains the scaling of $D(L)$ with the system size L by a simple match in the behavior of $s^2(L, t)$ across $T^* \sim L^{3/2}$.

V. LINEAR INTERFACE MODEL: ANALYTICAL RESULTS

The existence of size-dependent time scales in $\sigma^2(L, t)$ and $s^2(L, t)$ for the ASEP, discussed in this paper, can be explained qualitatively by exactly solving the continuum equation, Eq. 7, in the limit $\lambda \rightarrow 0$. This is possible as, in this limit, Eq. 7 is linear, and hence, solvable. We refer to the corresponding interface as a linear interface. The relevant time evolution equation is

$$\frac{\partial h(x, t)}{\partial t} = v_P + \Gamma \frac{\partial^2 h}{\partial x^2} + u \frac{\partial h}{\partial x} + \eta(x, t). \quad (26)$$

In this section, we outline the exact computation of the two quantities $\sigma^2(L, t)$ and $s^2(L, t)$ for the linear interface. We will see that the drift term, $u \frac{\partial h}{\partial x}$ in Eq. 26, that makes it different from the usual EW equation, plays a crucial role in determining the temporal behavior of these functions.

Our aim is to compute $\sigma^2(L, t)$ and $s^2(L, t)$ for the linear interface. For this, we look at the function $C_L(t_0, t_0 + t)$, defined in Eq. 5, which, utilizing the mapping outlined in Table I with n replaced by the continuous variable x , reads

$$C_L(t_0, t_0 + t) = \langle [h(x, t_0 + t) - h(x, t_0) - \langle [h(x, t_0 + t) - h(x, t_0)] \rangle]^2 \rangle. \quad (27)$$

As discussed in Section II, $\sigma^2(L, t)$ can be obtained from the limiting behavior of the function $C_L(t_0, t_0 + t)$ in the limit $t_0 \rightarrow \infty$. On the other hand, one recovers $s^2(L, t)$ from the limiting behavior of the function $C_L(t_0, t_0 + t)$ in the limit $t_0 \rightarrow 0$.

To compute $C_L(t_0, t_0 + t)$, we need to solve Eq. 26 for $h(x, t)$. Before doing so, we note that the constant term on the right of Eq. 26 can be gotten rid of by going to a co-moving frame moving with velocity v_P . This is equivalent to making the transformation $h \rightarrow h + v_P t$. The resultant equation is the usual time-evolution equation for the EW interface, Eq. 8, with an additional drift term,

$u \frac{\partial h}{\partial x}$, and can be solved by going to Fourier space. To this end, utilizing the boundary condition $h(x \pm L, t) = h(x, t)$ on the height variable, we write $h(x, t)$ in terms of its Fourier modes $\tilde{h}(m, t)$. We have

$$h(x, t) = \sum_{m=-\infty}^{\infty} \tilde{h}(m, t) e^{\frac{i2\pi m}{L}(x+ut)}. \quad (28)$$

Thus, $\tilde{h}(m, t) = \frac{1}{L} \int_0^L dx h(x, t) e^{-\frac{i2\pi m}{L}(x+ut)}$. Equation 26 now reads

$$\frac{\partial \tilde{h}(m, t)}{\partial t} = -\Gamma \frac{4\pi^2 m^2}{L^2} \tilde{h}(m, t) + \tilde{\eta}(m, t), \quad (29)$$

where $\tilde{\eta}(m, t) = \frac{1}{L} \int_0^L dx \eta(x, t) e^{-\frac{i2\pi m}{L}(x+ut)}$. Utilizing $\langle \eta(x, t) \eta(x', t') \rangle = 2A\delta(x-x')\delta(t-t')$, we have, for the Fourier modes,

$$\langle \tilde{\eta}(m, t) \tilde{\eta}(m', t') \rangle = \frac{2A}{L} \Delta_{m, -m'} \delta(t-t'), \quad (30)$$

where $\Delta_{m, n}$ is the Kronecker delta.

Equation 29 can be solved for $\tilde{h}(m, t)$ to get

$$\begin{aligned} \tilde{h}(m, t) &= \tilde{h}(m, 0) e^{-\Gamma \frac{4\pi^2 m^2}{L^2} t} \\ &+ e^{-\Gamma \frac{4\pi^2 m^2}{L^2} t} \int_0^t dt' \tilde{\eta}(m, t') e^{\Gamma \frac{4\pi^2 m^2}{L^2} t'}. \end{aligned} \quad (31)$$

The condition $\langle \eta(x, t) \rangle = 0$ gives, for its Fourier modes,

$\langle \tilde{\eta}(m, t) \rangle = 0 \forall m$. Using this in Eq. 31, we get $\langle \tilde{h}(m, t) \rangle = \langle \tilde{h}(m, 0) \rangle e^{-\Gamma \frac{4\pi^2 m^2}{L^2} t}$.

From Eq. 31, with the help of Eq. 30, we get

$$\begin{aligned} \langle \tilde{h}(m, t) \tilde{h}(m', t') \rangle &= \langle \tilde{h}(m, 0) \tilde{h}(m', 0) \rangle e^{-\Gamma \frac{4\pi^2}{L^2} (m^2 t + m'^2 t')} \\ &+ \frac{AL}{4\pi^2 \Gamma} \frac{\Delta_{m, -m'}}{m^2} \left[e^{-\Gamma \frac{4\pi^2 m^2}{L^2} |t-t'|} - e^{-\Gamma \frac{4\pi^2 m^2}{L^2} (t+t')} \right]. \end{aligned} \quad (32)$$

A. $\sigma^2(L, t)$

Here, we need to take the limit $t_0 \rightarrow \infty$ in the function $C_L(t_0, t_0 + t)$. Thus, we will compute

$$\sigma^2(L, t) = \lim_{t_0 \rightarrow \infty} C_L(t_0, t_0 + t) = \lim_{t_0 \rightarrow \infty} \langle [h(x, t_0 + t) - h(x, t_0) - \langle h(x, t_0 + t) - h(x, t_0) \rangle]^2 \rangle. \quad (33)$$

In the limit $t_0 \rightarrow \infty$, the quantity $\langle h(x, t_0 + t) - h(x, t_0) \rangle$ goes to zero. Thus, the function $\sigma^2(L, t)$ reduces to $\sigma^2(L, t) = \lim_{t_0 \rightarrow \infty} \langle [h(x, t_0 + t) - h(x, t_0)]^2 \rangle$.

Utilizing Eq. 32, we get

$$\begin{aligned} \langle h(x, t) h(x, t') \rangle &= \langle \tilde{h}^2(0, 0) \rangle + \frac{2A}{L} \min(t, t') \\ &+ \frac{AL}{4\pi^2 \Gamma} \sum_{m=-\infty, m \neq 0}^{\infty} \frac{1}{m^2} \left[e^{-\Gamma \frac{4\pi^2 m^2}{L^2} |t-t'|} - e^{-\Gamma \frac{4\pi^2 m^2}{L^2} (t+t')} \right] \\ &\quad \times e^{\frac{i2\pi mu}{L}(t-t')}. \end{aligned} \quad (34)$$

In the last equation, the contribution from the initial condition, $\langle \tilde{h}(m, 0) \tilde{h}(m', 0) \rangle e^{-\Gamma \frac{4\pi^2 m^2}{L^2} (m^2 t + m'^2 t')}$ for $m, m' \neq 0$ has been dropped, since, eventually when we set $t = t_0$ and $t' = t_0 + t$ and let $t_0 \rightarrow \infty$, this exponential term goes to 0. By combining the m and $-m$ terms in the summation in Eq. 34, we get

$$\begin{aligned} \langle h(x, t) h(x, t') \rangle &= \langle \tilde{h}^2(0, 0) \rangle + \frac{2A}{L} \min(t, t') \\ &+ \frac{AL}{2\pi^2 \Gamma} \sum_{m=1}^{\infty} \frac{1}{m^2} \left[e^{-\Gamma \frac{4\pi^2 m^2}{L^2} |t-t'|} - e^{-\Gamma \frac{4\pi^2 m^2}{L^2} (t+t')} \right] \\ &\quad \times \cos\left(\frac{2\pi mu}{L}(t-t')\right). \end{aligned} \quad (35)$$

Utilizing this expression in $C_L(t_0 + t, t_0)$, and then taking the limit $t_0 \rightarrow \infty$, we finally get

$$\sigma^2(L, t) = \frac{2A}{L} t + \frac{AL}{\pi^2 \Gamma} \sum_{m=1}^{\infty} \frac{1}{m^2} \left[1 - e^{-\Gamma \frac{4\pi^2 m^2}{L^2} t} \cos\left(\frac{2\pi mu}{L} t\right) \right]. \quad (36)$$

This is an exact formula for $\sigma^2(L, t)$ within the linear model. Next, we consider the various limits.

- $t \ll L/u$. Let $\frac{2\pi ut}{L} m = k$. With $\Delta m = 1$, we get $\Delta k = \frac{2\pi ut}{L}$. Now, $ut \ll L$ implies that Δk is small, and hence, one can replace the sum over m in Eq. 36 by an integral over k to get

$$\sigma^2(L, t) \approx \frac{2Aut}{\pi \Gamma} \int_0^{\infty} \frac{dk}{k^2} \left[1 - e^{-\frac{\Gamma k^2}{u^2 t}} \cos(k) \right], \quad (37)$$

where, in obtaining the last equation, we have dropped the first term on the right of Eq. 36 in comparison with the second term. The integral on the right can be done exactly, see Appendix C. Using its value, we get

$$\sigma^2(L, t) = \frac{Au}{\Gamma} \left[2 \frac{\sqrt{\Gamma}}{\sqrt{\pi} u} \sqrt{t} e^{-\frac{u^2 t}{4t}} + t \operatorname{erf}\left(\frac{u}{2\sqrt{\Gamma}} \sqrt{t}\right) \right]. \quad (38)$$

Now we consider two cases:

- (a) $t \ll \frac{4\Gamma}{u^2}$: In this limit, the error function is approximately zero, and we get

$$\sigma^2(L, t) \approx \frac{2A}{\sqrt{\pi \Gamma}} \sqrt{t}. \quad (39)$$

(b) $\frac{4\Gamma}{u^2} \ll t \ll \frac{L}{u}$. Here,

$$\sigma^2(L, t) \approx \frac{Au}{\Gamma} t. \quad (40)$$

- $t \sim \frac{L}{u}$: Let $t = \frac{nL}{u}$ with $n \in I$. Also, let $\frac{2\pi m\sqrt{\Gamma}}{\sqrt{uL}} = k$. Substituting in Eq. 36 after replacing, for large L , the sum over m by an integral over k , we get

$$\sigma^2(L, t = \frac{nL}{u}) \approx \frac{2At}{L} + \frac{2A}{\pi} \sqrt{\frac{L}{u\Gamma}} \int_0^\infty \frac{dk}{k^2} (1 - e^{-k^2 n}). \quad (41)$$

The integral on the right can be done exactly, and its value is $\sqrt{n\pi}$. This gives

$$\sigma^2(L, t = \frac{nL}{u}) \approx \frac{2A}{L} t + \frac{2A}{\sqrt{\pi\Gamma}} \sqrt{t}. \quad (42)$$

For large L , keeping t fixed, when the first term on the rhs goes to zero, we have

$$\sigma^2(L, t = \frac{nL}{u}) \approx \frac{2A}{\sqrt{\pi\Gamma}} \sqrt{t}. \quad (43)$$

- $t \gg L^2$: In this limit, the exponential term in the sum on the rhs of Eq. 36 drops out for all m to give

$$\begin{aligned} \sigma^2(L, t) &\approx \frac{2A}{L} t + \frac{AL}{\pi^2\Gamma} \sum_{m=1}^\infty \frac{1}{m^2} \\ &= \frac{2A}{L} t + \frac{AL}{\pi^2\Gamma} \left(\frac{\pi^2}{6} \right). \end{aligned} \quad (44)$$

In the limit of large t , the first term on the rhs dominates so that

$$\sigma^2(L, t) \approx \frac{2A}{L} t. \quad (45)$$

Note that the large time behavior of $\sigma^2(L, t)$ is determined by the zero mode ($m = 0$) in the Fourier expansion of $h(x, t)$.

With the values of the exponents β and z for EW given in Eq. 12, we summarize the behavior of $\sigma^2(L, t)$ for the linear interface in Table II.

The scaling of the diffusion constant $D(L)$ as the inverse of the system size in the regime $t \gg T_2 \sim L^z$ with $z = z_{EW} = 2$ can be obtained by matching the behavior of the $\sigma^2(L, t)$ across the time T_2 .

Let $\sigma^2(L, t) \sim D(L)t$ with $D(L) \sim L^\gamma$ for $t \gg T_2$.

On the lower side of T_2 , we have $\sigma^2(L, t) \sim t^{2\beta}$.

Then, to match the t and L dependence at T_2 , we must have

$$(T_2)^{2\beta} \sim D(L)T_2. \quad (46)$$

This gives $2\beta = \gamma/z + 1$ whence, with $z = 2$ and $\beta = 1/4$ for the linear model, $\gamma = -1$.

$t \ll T_1 \sim L:$	
(a) $t \ll \frac{4\Gamma}{u^2}.$	$\sigma^2(L, t) \approx \frac{2A}{\sqrt{\pi\Gamma}} \sqrt{t}.$
(b) $\frac{4\Gamma}{u^2} \ll t \ll T_1.$	$\sigma^2(L, t) \approx \frac{Au}{\Gamma} t.$
$T_1 \ll t \ll T_2 \sim L^z.$	$\sigma^2(L, t) \approx \frac{2A}{\sqrt{\pi\Gamma}} t^{2\beta}.$
$z = z_{EW} = 2.$	$\beta = \beta_{EW} = 1/4.$
$t = \frac{nL}{u}$ with $n \in I.$	
$t \gg T_2.$	$\sigma^2(L, t) \approx \frac{2A}{L} t.$
	The diffusion constant $D(L) = \frac{2A}{L}.$

TABLE II: Behavior of $\sigma^2(L, t)$ in different time regimes for the linear interface.

$t \ll T_1 \sim L:$	
(a) $t \ll \frac{4\Gamma}{u^2}.$	$\sigma^2(L, t) \sim \sqrt{t}.$
(b) $\frac{4\Gamma}{u^2} \ll t \ll T_1.$	$\sigma^2(L, t) \sim t.$
$T_1 \ll t \ll T_2 \sim L^z.$	$\sigma^2(L, t) \sim t^{2\beta}.$
$z = z_{KPZ} = 3/2.$	$\beta = \beta_{KPZ} = 1/3.$
$t = \frac{nL}{u}$ with $n \in I.$	
$t \gg T_2.$	$\sigma^2(L, t) \sim \frac{1}{\sqrt{L}} t.$
	The diffusion constant $D(L) \sim 1/\sqrt{L}.$

TABLE III: Behavior of $\sigma^2(L, t)$ in different time regimes for the KPZ interface.

On the basis of the above results for the linear model, we expect the time-dependence of $\sigma^2(L, t)$ for the KPZ class as in Table III. Here, $z = z_{KPZ} = 3/2$ and $\beta = \beta_{KPZ} = 1/3$ so that $\gamma = -1/2$. This value for γ leads to the inverse square root scaling of the diffusion constant $D(L)$ with system size L .

B. $s^2(L, t)$

Here, we need to take $t_0 \rightarrow 0$ in the function $C_L(t_0, t_0 + t)$. Thus, we will compute

$$\begin{aligned} s^2(L, t) &= \lim_{t_0 \rightarrow 0} C_L(t_0, t_0 + t) \\ &= \langle [h(x, t) - h(x, 0) - \langle [h(x, t) - h(x, 0)] \rangle]^2 \rangle. \end{aligned} \quad (47)$$

Now, from Eq. 31, we have

$$\begin{aligned} h(x, t) - h(x, 0) &= \sum_{m=-\infty}^\infty [\tilde{h}(m, 0) e^{-\Gamma \frac{4\pi^2 m^2}{L^2} t} + \\ &e^{-\Gamma \frac{4\pi^2 m^2}{L^2} t} \int_0^t dt' \tilde{\eta}(m, t') e^{\Gamma \frac{4\pi^2 m^2}{L^2} t'}] \times e^{\frac{i2\pi m}{L}(x+ut)} \\ &\quad - \sum_{m=-\infty}^\infty \tilde{h}(m, 0) e^{\frac{i2\pi m}{L} x}. \end{aligned} \quad (48)$$

Noting that every time we start from the same initial condition so that $\langle \tilde{h}(m, 0) \rangle = \tilde{h}(m, 0)$, we have

$$h(x, t) - h(x, 0) - \langle [h(x, t) - h(x, 0)] \rangle =$$

$$\sum_{m=-\infty}^{\infty} e^{-\Gamma \frac{4\pi^2 m^2}{L^2}} e^{\frac{i2\pi m}{L}(x+ut)} \int_0^t dt' \tilde{\eta}(m, t') e^{\Gamma \frac{4\pi^2 m^2}{L^2} t'}. \quad (49)$$

Utilizing Eq. 49 and Eq. 30 in Eq. 47, we get, after a few steps,

$$s^2(L, t) = \frac{AL}{4\pi^2\Gamma} \sum_{m=-\infty}^{\infty} \frac{1}{m^2} (1 - e^{-\Gamma \frac{8\pi^2 m^2}{L^2} t}). \quad (50)$$

Separating out the $m = 0$ mode and exploiting the $m \rightarrow -m$ symmetry of the remaining terms, we get the final expression for $s^2(L, t)$ as

$$s^2(L, t) = \frac{2A}{L}t + \frac{AL}{2\pi^2\Gamma} \sum_{m=1}^{\infty} \frac{1}{m^2} (1 - e^{-\Gamma \frac{8\pi^2 m^2}{L^2} t}). \quad (51)$$

Next, we will consider the various limits.

- $t \ll L^2$: Let $k = \frac{2\sqrt{2}\Gamma\pi m}{L}\sqrt{t}$. Since $\Delta m = 1$, we have $\Delta k = \frac{2\sqrt{2}\Gamma\pi}{L}\sqrt{t}$ is small for $t \ll L^2$. This allows the sum over m in Eq. 51 to be replaced by an integral over k to give

$$s^2(L, t) = \frac{2A}{L}t + \frac{A}{\pi} \sqrt{\frac{2}{\Gamma}} \sqrt{t} \int_{\frac{2\sqrt{2}\Gamma\pi\sqrt{t}}{L}}^{\infty} \frac{dk}{k^2} (1 - e^{-k^2}). \quad (52)$$

Since $t \ll L^2$, the lower limit of the integral on the right can be taken to be 0. Then the integral can be done exactly, and its value is $\sqrt{\pi}$. For large L , keeping t fixed, the first term on the right of Eq. 52 goes to zero, and we get

$$s^2(L, t) \approx A \sqrt{\frac{2}{\pi\Gamma}} \sqrt{t}. \quad (53)$$

- $t \gg L^2$: In this limit, the exponential term in the sum on the rhs of Eq. 51 gets damped out for all m so that we finally have

$$\begin{aligned} s^2(L, t) &\approx \frac{2A}{L}t + \frac{AL}{2\pi^2\Gamma} \sum_{m=1}^{\infty} \frac{1}{m^2} \\ &= \frac{2A}{L}t + \frac{AL}{2\pi^2\Gamma} \left(\frac{\pi^2}{6} \right). \end{aligned} \quad (54)$$

For large t , the first term on the rhs dominates so that

$$s^2(L, t) \approx \frac{2A}{L}t. \quad (55)$$

Here, as for the function $\sigma^2(L, t)$, we see that the large time behavior of $s^2(L, t)$ is determined by the zero mode ($m = 0$) in the Fourier expansion of $h(x, t)$.

$t \ll T^* \sim L^z$.	$s^2(L, t) \approx Ct^{2\beta}$.
$z = z_{EW} = 2$.	$\beta = \beta_{EW} = 1/4$.
	$C = A\sqrt{\frac{2}{\pi\Gamma}}$.
$t \gg T^*$.	$s^2(L, t) \approx \frac{2A}{L}t$.
$z = z_{EW} = 2$.	The diffusion constant $D(L) = \frac{2A}{L}$.

TABLE IV: Behavior of $s^2(L, t)$ in different time regimes for the linear interface.

Knowing the values of the exponents β and z for EW, given in Eq. 12, we summarize the behavior of $s^2(L, t)$ for the linear interface in Table IV. The fact that $D(L)$ scales as the inverse of the system size in the regime $t \gg T^* \sim L^z$ with $z = z_{EW} = 2$, can be obtained by matching the behavior of $s^2(L, t)$ across the time T^* .

Thus, let $s^2(L, t) \sim D(L)t$ with $D(L) \sim L^\gamma$ for $t \gg T^*$. For $t \ll T^*$, we have $s^2(L, t) \sim t^{2\beta}$.

Then, to match the t and L dependence at T^* , we must have

$$(T^*)^{2\beta} \sim D(L)T^*. \quad (56)$$

This gives $2\beta = \gamma/z + 1$. With $\beta = 1/4$ and $z = 2$ for the linear model, $\gamma = -1$.

The above results lead us to expect the time-dependence of $s^2(L, t)$ for the KPZ class as in Table V.

$t \ll T^* \sim L^z$.	$s^2(L, t) \sim t^{2\beta}$.
$z = z_{KPZ} = 3/2$.	$\beta = \beta_{KPZ} = 1/3$.
$t \gg T^*$.	$s^2(L, t) \sim \frac{1}{\sqrt{L}}t$.
	The diffusion constant $D(L) \sim 1/\sqrt{L}$.

TABLE V: Behavior of $s^2(L, t)$ in different time regimes for the KPZ interface.

Here, $\beta = \beta_{KPZ} = 1/3$ and $z = z_{KPZ} = 3/2$ so that $2\beta = \gamma/z + 1$ gives $\gamma = -1/2$. This explains the inverse square root scaling of the diffusion constant $D(L)$ with system size L .

Note that from Table V, it follows that for an infinite system when the time-scale T^* diverges, one recovers the result observed by van Beijeren that $\lim_{L \rightarrow \infty} s^2(L, t) = s^2(t) \sim t^{2/3}$ [4].

To conclude this section, we reiterate that the exact solution for the linear interface qualitatively explains the occurrence of characteristic oscillations and different L -dependent regimes in the variance of the displacement on a finite lattice, as observed, for instance, in the Monte Carlo simulations for the ASEP. We also note that in the large time limit ($t \gg L^z$ with $z = 3/2$ for the ASEP and $z = 2$ for the linear interface), both $\sigma^2(L, t)$ and $s^2(L, t)$ grow linearly in time with the same constant of proportionality or the diffusion constant $D(L)$. For the linear interface, $D(L) \sim \frac{1}{L}$, while $D(L) \sim \frac{1}{\sqrt{L}}$ for the ASEP.

VI. CORRESPONDENCE OF THE LINEAR MODEL TO DIFFERENT INTERACTING PARTICLE SYSTEMS

The evolution equation, Eq. 26, in addition to being a linear approximation to the KPZ equation with a drift term, also arises in a number of microscopic interacting particle systems. Examples are the Katz-Lebowitz-Spohn (KLS) model at a specified value of the temperature, and the Asymmetric Random Average Process (ARAP). These correspondences are discussed below.

A. Correspondence to the KLS model

The aim of this subsection is to explain how the variance of the displacement, computed in the linearized continuum theory and defined in terms of the macroscopic parameters (Γ , A , speed u), compares to the same quantity evaluated by numerical simulations in the (discrete) KLS model, which uses one single microscopic parameter, namely, the temperature, for a special value of the latter.

1. KLS model: a reminder

The one-dimensional KLS model generalizes the ASEP, in that interactions between particles are added on top of the exclusion constraint [16]. The ASEP is the infinite temperature limit of the KLS model.

The precise definition of the KLS model is as follows. Consider a chain of Ising spins s_n ($n = 1, \dots, N$), evolving under the Kawasaki dynamics with the heat-bath rule, and submitted to a drift. The energy of the chain reads

$$E = -\tilde{J} \sum_n s_n s_{n+1}. \quad (57)$$

In the heat-bath dynamics, for a pair of opposite spins ($s_n + s_{n+1} = 0$), the move ($s_n \rightarrow -s_n, s_{n+1} \rightarrow -s_{n+1}$) is realized with probability

$$W(\Delta E) = \frac{\mathcal{P}}{e^{\beta \Delta E} + 1}, \quad (58)$$

where $\Delta E = 2\tilde{J}(s_{n-1}s_n + s_{n+1}s_{n+2}) = 0, \pm 4\tilde{J}$ is the energy difference between the configurations after and before the move, and the numerator \mathcal{P} is taken equal to p if the $+$ spin is exchanged to the right (i.e., $+- \rightarrow -+$), and to q if it is exchanged to the left ($-+ \rightarrow +-$). Associating a particle to a $+$ spin, and a hole to a $-$ spin, this particle hops to the right with probability p , and to the left with probability q .

The moves corresponding to the three possible values of the difference ΔE are listed in the Table VI, with the corresponding acceptance probabilities. Evaporation corresponds to the detachment of a $+$ spin from a positive

domain, or, equivalently, to the detachment of a particle from a cluster of particles. Condensation, conversely, corresponds to the attachment of an isolated $+$ spin to a positive domain, or, equivalently, to that of a particle to a cluster of particles, and the two diffusion mechanisms, to the motion of an isolated $-$ spin in a positive domain (or hole in a cluster of particles) or to that of an isolated $+$ spin in a negative domain (or particle amongst empty sites).

The heat-bath rule, Eq. 58, has the non-trivial property that the steady state is independent of the asymmetry [16, 32]. It obeys detailed balance with respect to the energy, Eq. 57, at temperature $T = 1/(k_B\beta)$ (k_B : Boltzmann constant), i.e., $W(\Delta E) = W(-\Delta E)e^{-\beta\Delta E}$.

Type	ΔE	Acceptance Prob.	Moves
Condensation	$-4\tilde{J}$	$\mathcal{P} e^{4\beta\tilde{J}} / (e^{4\beta\tilde{J}} + 1)$	$- + - + \rightarrow - - + +$ $+ - + - \rightarrow + + - -$
Diffusion	0	$\mathcal{P}/2$	$+ + - + \leftrightarrow + - + +$ $- - + - \leftrightarrow - - + -$
Evaporation	$+4\tilde{J}$	$\mathcal{P} / (e^{4\beta\tilde{J}} + 1)$	$+ + - - \rightarrow + - + -$ $- - + + \rightarrow - - + +$

TABLE VI: Types of moves in the partially asymmetric Kawasaki dynamics, and corresponding acceptance probabilities with the heat-bath rule. The probability \mathcal{P} is equal to p when the $+$ spin exchanges to the right, to q when it exchanges to the left.

The KLS model can also be viewed as a migration process (or urn model). Generally speaking, a migration process can be seen as a generalization of the Zero Range Process (ZRP) [33, 34], where the particles hop on a lattice, but where the hopping rate depends both on the departure and arrival sites [35, 34]. Particles (or $+$ spins) are identified with the sites of a lattice, and the holes (or $-$ spins) with particles located on these sites. At infinite temperature, this maps the ASEP onto the usual ZRP. At finite temperature, the rate at which a particle hops to the neighboring site is still given by Eq. 58 with $\Delta E = -4\delta\tilde{J}$ where δ is the variation of the number of empty sites before and after moving the particle. This mapping is effectively used in numerical simulations.

2. The variance of the displacement

The displacement of a tagged particle in the KLS model obeys the same laws as for the ASEP, i.e., all phenomena presented in this paper for the ASEP exist likewise for the KLS model. More precisely, the temporal behavior of the variance of the displacement of the tagged particle is the same as for the ASEP, up to prefactors which depend continuously on the temperature. The question is now to make a link between the microscopic model and its continuum limit description, i.e., to compare the prediction of Section V for the temporal evolution of the variance, in the linear theory, to numerical simulations of the model.

For that purpose, we will (i) express the parameters of the continuum theory (Γ , A , and u) in terms of the temperature, which is the only parameter of the KLS model, (ii) explain the relevance of the linear theory for a special value of the temperature, for which the coefficient of the nonlinear term in the KPZ equation vanishes. This identification is possible in the present case because the stationary state of the KLS model is known. The method is given in [36]. It needs to be slightly generalized here, as now explained. For the sake of simplicity, we will restrict the computations to the case of zero magnetization M , or, equivalently, of density $\rho = 1/2$ (since $M = 2\rho - 1$).

First, the following relationship between the diffusion constant Γ and the strength of the noise A , is always valid, independently of the asymmetry [36],

$$A = \Gamma \chi, \quad (59)$$

$$\begin{aligned} J_n^{sp} = & \frac{p-q}{4} \left(1 - \langle s_{n-1} s_n \rangle + \frac{e^{4\beta\bar{J}} - 1}{2(e^{4\beta\bar{J}} + 1)} \langle (s_n - s_{n-1})(s_{n-2} - s_{n+1}) \rangle \right) \\ & + \frac{1}{4} \left(\langle s_{n-1} \rangle - \langle s_n \rangle + \frac{e^{4\beta\bar{J}} - 1}{2(e^{4\beta\bar{J}} + 1)} (\langle s_{n+1} \rangle - \langle s_{n-2} \rangle + \langle s_{n-2} s_{n-1} s_n \rangle - \langle s_{n-1} s_n s_{n+1} \rangle) \right). \end{aligned} \quad (61)$$

The first line in Eq. 61 is the drift term. It is only present when the dynamics is asymmetric. It does not contribute to the computation of the diffusion constant Γ . Putting aside the drift term, the right-hand side of Eq. 61 appears as a second order difference, consistently with the diffusive nature of the second term. (Note also that the first term is even in the spin variable, while the second one is odd.) In other words, the expression of Γ is the same both in the symmetric (EW) or asymmetric (KPZ) cases. It reads (see [36] for the computation)

$$\Gamma = \frac{1}{(e^{2\beta\bar{J}} + 1)(e^{4\beta\bar{J}} + 1)}. \quad (62)$$

Note that this expression differs by a factor 2 with that given in [36]. This is due to the difference in the definitions of the scale of time chosen in the present work (see Table VI), and in [36]. Utilizing Eq. 59 and the fact that the susceptibility $\chi = e^{2\beta\bar{J}}$, we get

$$A = \frac{1}{(e^{-2\beta\bar{J}} + 1)(e^{4\beta\bar{J}} + 1)}. \quad (63)$$

where χ is the susceptibility, explicitly known for the Ising chain, $\chi = e^{2\beta\bar{J}}$. In order to find an expression of Γ and of the speed of the tagged particle, we write the equation for the temporal evolution of the magnetization $\langle s_n \rangle$. This reads

$$\frac{d\langle s_n \rangle}{dt} = J_n^{sp} - J_{n+1}^{sp}, \quad (60)$$

where the spin current J_n^{sp} through the link $(n-1, n)$ has the following expression.

It remains to evaluate the speed u , as well as the coefficient of nonlinearity λ , appearing in the KPZ equation, Eq. 7. We use Eqns. B11 and B12 for this purpose. Now, without loss of generality, we consider completely asymmetric particle (i.e., + spin) motion with $p = 1$ and $q = 0$. For zero magnetization (or, equivalently, at density $\rho = 1/2$), since u is given by $u = \left[v_P - \frac{\partial J}{\partial \rho} \right] \Big|_{\rho=1/2} = \left[v_P - 2 \frac{\partial J}{\partial M} \right] \Big|_{M=0}$, while λ is given by $\lambda = 2 \frac{\partial^2 J}{\partial M^2} \Big|_{M=0}$, we need to evaluate the current of particles J as a function of the magnetization M . Note that $J = J^{sp}/2$. We use Eq. 61, with $\langle s_n \rangle = M$, $\langle s_n s_{n+1} \rangle = \langle s_1 s_2 \rangle$, by translation invariance, etc. Hence the current reads

$$J = \frac{1}{8} \left(1 + \frac{e^{4\beta\bar{J}} - 1}{e^{4\beta\bar{J}} + 1} \langle s_1 s_3 \rangle - \frac{2e^{4\beta\bar{J}}}{e^{4\beta\bar{J}} + 1} \langle s_1 s_2 \rangle \right). \quad (64)$$

The correlators are known by the transfer matrix method which gives J as [36]

$$J = \frac{2M^2 + e^{4\beta\bar{J}}(1 - M^2) - (1 + M^2)(M^2 + e^{4\beta\bar{J}}(1 - M^2))^{1/2}}{2(e^{8\beta\bar{J}} - 1)(1 - M^2)}. \quad (65)$$

Utilizing the last equation, we finally get

$$u = v_P = 2J|_{M=0} = \frac{e^{2\beta\bar{J}}}{(e^{2\beta\bar{J}} + 1)(e^{4\beta\bar{J}} + 1)}, \quad (66)$$

while

$$\lambda = \frac{1 - 3e^{2\beta\bar{J}}}{e^{2\beta\bar{J}}(e^{2\beta\bar{J}} + 1)(e^{4\beta\bar{J}} + 1)}. \quad (67)$$

Hence for $e^{-2\beta\tilde{J}} = 3$ (antiferromagnetic chain), λ vanishes. For such a value of the “temperature” (actually of $\beta\tilde{J}$), though the dynamics is asymmetric, the continuum theory is linear. This yields

$$\Gamma = \frac{27}{40}, \quad u = \frac{9}{40}, \quad A = \frac{9}{40}. \quad (68)$$

Note that the unit of time is such that at infinite temperature

$$\Gamma = \frac{1}{4}, \quad u = \frac{1}{4}, \quad A = \frac{1}{4}. \quad (69)$$

These quantities differ by a factor 2 from their expression for the SEP (see Appendix B). As above, the origin of this difference lies in the definitions of the scale of time for these two models (see Table VI).

The result of the comparison of the quantity $\sigma^2(L, t)$ as obtained from simulation of the KLS model on a ring of size L for the temperature T satisfying $e^{-2\beta\tilde{J}} = 3$, and that from the exact solution of the linear interface as given in Eq. 36 (with the corresponding values of the constants Γ, A and u given in Eq. 68) is shown in Fig. 8 for three different system sizes ($L = 64, 128, 256$). The simulation of the KLS model was done in the equivalent migration process described above, with equal number of particles and sites, which corresponds to half filling ($\rho = 1/2$) in the original particle system (i.e. the KLS model). The variance of the displacement of a given tagged particle in the KLS model translates into the variance of the number of particles which passed through a given bond in the migration process.

B. Correspondence to the ARAP

The Asymmetric Random Average Process involves hard core particles hopping on a real line as opposed to a lattice for the ASEP [17]. We consider a system of particles of average density ρ . We denote by $x_i(t)$ the location of the i -th particle on the real line with periodic boundary conditions. The dynamics is stochastic and involves the following moves during an infinitesimal time dt : a randomly chosen particle jumps with probability pdt to the right, with probability qdt to the left, and with probability $1 - (p+q)dt$, it continues to occupy its original location. The amount by which the particle moves either to the right or to the left is a random fraction of the gap to the next particle to the right or to the left. Thus, for the i -th particle, the jump to the right is by the amount $r_i^+(x_{i+1} - x_i)$, while to the left is by the amount $r_i^-(x_i - x_{i-1})$. Here, the random variables r_i^\pm are independently drawn from the interval $[0, 1]$, each being distributed according to the same pdf $f(r)$, which is arbitrary. The time evolution equation of the positions x_i 's is represented by the exact Langevin equation

$$x_i(t + dt) = x_i(t) + \gamma_i(t), \quad (70)$$

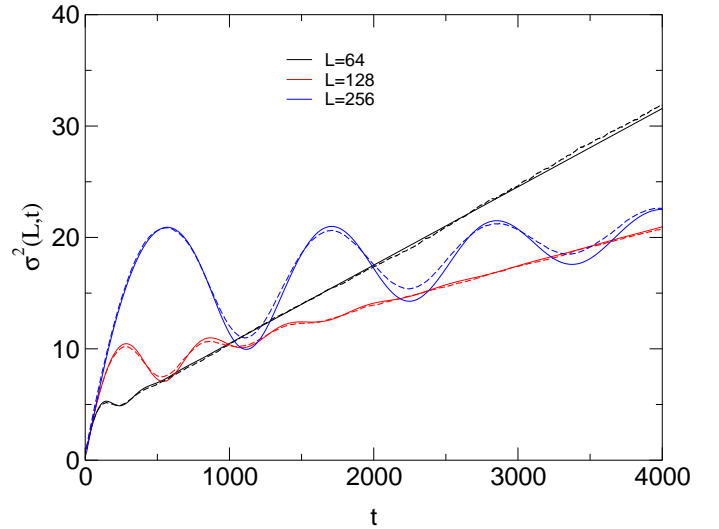


FIG. 8: (Color online) Comparison of the variance $\sigma^2(L, t)$ of the displacement of the tagged particle in the KLS model obtained from simulations (dashed lines) and exact solution (full lines) of the corresponding continuum linear theory for the temperature T satisfying $e^{-2\tilde{J}/k_B T} = 3$. Results are shown for three different system sizes ($L = 64, 128, 256$). Simulation of the KLS model is done with the equivalent migration process.

where the random variables $\gamma_i(t)$ are given by

$$\gamma_i(t) = \begin{cases} r_i^+ [x_{i+1}(t) - x_i(t)] & \text{with prob. } pdt, \\ r_i^- [x_{i-1}(t) - x_i(t)] & \text{with prob. } qdt, \\ 0 & \text{with prob. } 1 - (p+q)dt. \end{cases} \quad (71)$$

The average velocity of a tagged particle v_P is given by

$$v_P = \frac{d\langle x_i(t) \rangle}{dt} = \langle \gamma_i(t) \rangle. \quad (72)$$

Using the expression for γ_i in Eq. 71, we can compute its average. This gives the average velocity of an ARAP particle as $v_P = \frac{(p-q)\mu_1}{\rho}$, where $\mu_1 = \int_0^1 dr r f(r)$. Thus the average particle current $J = \rho v_P$ is independent of ρ . The derivation of the corresponding interface equation can be done along the lines outlined in Appendix B. Noting that all derivatives of J with respect to ρ are zero, Eq. B11 implies $u = v_P$, while $\lambda = 0$ from Eq. B12. Thus, we recover the equation for the linear interface, Eq. 26. Based on our exact solution for the linear interface, we expect the tagged-particle correlation in the ARAP on an infinite system as measured by $\sigma^2(t) \equiv \lim_{L \rightarrow \infty} \sigma^2(L, t)$ to vary as t (cf. Table II). This has been confirmed by an exact solution of the tagged-particle correlation for the ARAP on an infinite system [37].

VII. CENTER-OF-MASS MOTION

In this section, we examine the motion of the center-of-mass for the ASEP, defined as

$$Y_{CM}(t) = \frac{1}{N} \sum_{n=1}^N y(n, t). \quad (73)$$

Define, for fixed initial configuration, drawn from the stationary ensemble,

$$d_{CM}(t) = Y_{CM}(t) - Y_{CM}(0) - \langle Y_{CM}(t) - Y_{CM}(0) \rangle, \quad (74)$$

where, as usual, angular brackets denote averaging over noise in the evolution of configurations. On the basis of the representation in Eq. 14, we have

$$y(n, t) - y(n, 0) - \langle y(n, t) - y(n, 0) \rangle = t^\beta [\chi_n(t) - \langle \chi_n(t) \rangle]. \quad (75)$$

This gives

$$d_{CM}(t) = \frac{t^\beta}{N} \sum_{n=1}^N [\chi_n(t) - \langle \chi_n(t) \rangle]. \quad (76)$$

Hence,

$$\langle d_{CM}^2(t) \rangle = \frac{t^{2\beta}}{N^2} \sum_{n,m} [\langle \chi_n(t) \chi_m(t) \rangle - \langle \chi_n(t) \rangle \langle \chi_m(t) \rangle]. \quad (77)$$

The bracketed quantity on the right hand side, in the stationary state, becomes a function, $f(n-m, t)$, of the difference. Putting this in Eq. 77, we get

$$\langle d_{CM}^2(t) \rangle = \frac{t^{2\beta}}{N} \sum_{n-m} f(n-m, t). \quad (78)$$

The random variables $\chi_n(t)$ are correlated only up to $\xi(t) \sim t^{1/z}$. We write

$$\sum_{n-m} f(n-m, t) = \rho \int_0^{\xi(t)} dx f(x, t) \sim \rho t^{1/z} \int_0^1 dy g(y). \quad (79)$$

In arriving at the second step in the above equation, we have made a transformation of the tag variable ($n-m$) to the spatial variable x . Plugging Eq. 79 in Eq. 78, we get

$$\langle d_{CM}^2(t) \rangle \sim \frac{t^{2\beta+1/z}}{L}. \quad (80)$$

The above result is derived on the basis of the representation for the tagged particle displacement, Eq. 14, based on a scaling argument. Using the mapping in Table I, Eq. 80 is expected to hold for an interface with nonequilibrium dynamics with critical exponents β and z for times $t \ll L^z$. For large times $t \gg L^z$, the fluctuations are expected to grow diffusively, as indicated by the linear behavior of the variances $\sigma^2(L, t)$ and $s^2(L, t)$. Thus, for

$t \gg L^z$, we expect $\langle d_{CM}^2(t) \rangle \sim D(L)t$. Matching the behavior of $\langle d_{CM}^2(t) \rangle$ at the crossover time $t^* \sim L^z$, we get $D(L) \sim L^{(2\beta-1)z}$.

With $z = z_{KPZ} = 3/2$ and $\beta = \beta_{KPZ} = 1/3$ for the ASEP, we have

$$\langle d_{CM}^2(t) \rangle \sim \begin{cases} \frac{t^{4/3}}{L} & \text{if } t \ll L^{3/2} \\ \frac{t}{\sqrt{L}} & \text{if } t \gg L^{3/2}. \end{cases} \quad (81)$$

The result $\langle d_{CM}^2(t) \rangle \sim \frac{t^{4/3}}{L}$ for $t \ll L^{3/2}$ for the ASEP has already been observed by van Beijeren et al. in [38].

For the linear interface in the EW class with $\beta = \beta_{EW} = 1/4$, $z = z_{EW} = 2$, we get $D(L) \sim \frac{1}{L}$. Thus, for the linear interface, we expect, on the basis of our representation for the tagged particle displacement Eq. 14,

$$\langle d_{CM}^2(t) \rangle \sim \frac{t}{L} \quad (82)$$

for all times. Indeed, the above result, based on scaling arguments, is borne out by an exact computation of the quantity $\langle d_{CM}^2(t) \rangle$ for the linear interface model. Using the mapping of the ASEP to the interface in Table I, for an interface of length L , we get

$$d_{CM}(t) = \frac{1}{L} \int_0^L dx [h(x, t) - h(x, 0) - \langle [h(x, t) - h(x, 0)] \rangle]. \quad (83)$$

We have $\tilde{h}(m, t) = \frac{1}{L} \int_0^L dx h(x, t) e^{-i \frac{2\pi m}{L}(x+ut)}$. This gives $\tilde{h}(0, t) = \frac{1}{L} \int_0^L dx h(x, t)$. Substituting in Eq. 83, we get

$$d_{CM}(t) = \tilde{h}(0, t) - \tilde{h}(0, 0) - \langle [\tilde{h}(0, t) - \tilde{h}(0, 0)] \rangle. \quad (84)$$

Using Eq. 31, we finally get

$$d_{CM}(t) = \int_0^t dt' \tilde{\eta}(0, t') \quad (85)$$

so that

$$\begin{aligned} \langle d_{CM}^2(t) \rangle &= \int_0^t \int_0^t dt' dt'' \langle \tilde{\eta}(0, t') \tilde{\eta}(0, t'') \rangle \\ &= \frac{2At}{L}, \end{aligned} \quad (86)$$

where we have used Eq. 30 in arriving at the last equation. This exact result matches with the one obtained on the basis of scaling arguments in Eq. 82.

VIII. CONCLUSION

In this paper, we have revisited the problem of tagged particle correlation in the ASEP in one dimension, with particular emphasis on finite size effects. The stationary state variance of the displacement of a tagged particle involves averaging with respect to an initial stationary

ensemble and stochastic evolution. This quantity shows two distinct size-dependent time scales, $T_1 \sim L$, and $T_2 \sim L^{3/2}$. The behavior is linear for both the time regimes $t \ll T_1$ and $t \gg T_2$, while for intermediate times $T_1 \ll t \ll T_2$, the variance $\sigma^2(L, t)$ shows pronounced oscillations with a well-defined size-dependent time period. We understand the oscillations as arising from the sliding density fluctuations (SDF) relative to the drift of the tagged particle in the stationary state, the density fluctuations themselves being transported through the system by kinematic waves.

Following van Beijeren [4], we also study the variance $s^2(L, t)$ of the displacement of the tagged particle by averaging with respect to only stochastic evolution of a fixed initial configuration, drawn from the ensemble of stationary states. We see that the quantity $s^2(L, t)$ has only one time scale $T^* \sim L^{3/2}$. The variance $s^2(L, t)$ grows linearly in time for times $t \gg T^*$, while for times $t \ll T^*$, it grows as $t^{2/3}$.

Through a mapping to an interface, the time evolution equation for the stationary state ASEP density profile maps onto that for a nonequilibrium interface in the Kardar-Parisi-Zhang (KPZ) universality class of interface dynamics. This equation is nonlinear and cannot be solved exactly. By dropping the nonlinear term, we obtain a linear model in the Edwards-Wilkinson (EW) universality class, which we solve exactly. This exact solution was helpful in understanding the occurrence of size-dependent time-scales T_1 , T_2 and T^* , besides explaining the scaling properties of two other interacting particle systems.

IX. ACKNOWLEDGMENTS

We acknowledge useful discussions with H. van Beijeren, G. Schütz and J. M. Luck. We are grateful to the Isaac Newton Institute, Cambridge, UK, where many of these discussions took place during the workshop ‘Principles of the Dynamics of Non-Equilibrium Systems’, for its warm hospitality. MB’s stay at the Newton Institute was supported through EPSRC Grant 531174. MB and SNM acknowledge the support of the Indo-French Centre for the Promotion of Advanced Research (IFCPAR) under Project 3404-2. SG is grateful to the Kanwal Rekhi Career Development Fund for partial financial support.

APPENDIX A: A PRIMER ON KINEMATIC WAVES

The notion of kinematic waves goes back to the work of Lighthill and Whitham, who showed how their occurrence follows from the continuity equation. We briefly recapitulate their argument [8, 39] here.

The steady state coarse-grained density fluctuation,

$\delta\rho = \rho - \langle \rho \rangle$, satisfies the equation of continuity

$$\frac{\partial(\delta\rho)}{\partial t} = -\frac{\partial j}{\partial x}, \quad (\text{A1})$$

where j is the particle current. Assuming that j depends on x through its dependence on a space-varying density ρ , the above equation can be recast into

$$\frac{\partial\rho}{\partial t} = -c(\rho)\frac{\partial\rho}{\partial x}, \quad (\text{A2})$$

where $c(\rho) = \frac{\partial j}{\partial \rho}$. To lowest order in $\delta\rho$, Eq. A2 gives

$$\frac{\partial\rho}{\partial t} = -v_K\frac{\partial\rho}{\partial x} \quad (\text{A3})$$

with $v_K = c(\langle \rho \rangle)$. To leading order in $\delta\rho$, we have $v_K = \frac{\partial J}{\partial \rho}$, where J is the mean current in the steady state. Equation A3 is the familiar wave equation in one dimension, and the solution reads $\delta\rho = g(x - v_K t)$. Here, g is an arbitrary function of its argument. Thus, to leading order in $\delta\rho$, the solution to the equation of continuity gives kinematic waves of velocity v_K that transport density fluctuations through the system in the stationary state. The attribute ‘kinematic’ emphasizes the purely kinematic origin of these waves, in contrast to the dynamic origin of say, elastic and acoustic waves. v_K is identical to the collective velocity discussed in [40]. Note that this description neglects higher order terms in $\delta\rho$, which is tantamount to neglecting dissipation in the density profile while it is being bodily transported by the kinematic waves.

APPENDIX B: DERIVATION OF THE INTERFACE EQUATION

Here, we derive the interface equation, Eq. 7, following [41].

The local interparticle distance in the ASEP is given by

$$\frac{1}{\rho(x, t)} = \frac{\partial y}{\partial x}, \quad (\text{B1})$$

where $y(x, t)$ is the position of the x -th particle at time t . Now,

$$y(x, t) = \frac{x}{\rho} + h(x, t), \quad (\text{B2})$$

where ρ is the mean density of particles and $h(x, t)$ is the displacement of the x -th particle from the position it would have had, had the particles been uniformly placed. Then, we have $\rho(x, t)^{-1} = \rho^{-1} + \frac{\partial h}{\partial x}$, implying

$$\rho(x, t) = \frac{\rho}{1 + \rho \frac{\partial h}{\partial x}}. \quad (\text{B3})$$

Expanding in a power series in $\frac{\partial h}{\partial x}$,

$$\rho(x, t) = \rho - \rho^2 \frac{\partial h}{\partial x} + \rho^3 \left(\frac{\partial h}{\partial x} \right)^2 + \dots \quad (\text{B4})$$

The above equation can be rewritten as

$$\rho(x, t) = \rho + \psi(x, t) \text{ where } \psi(x, t) = -\rho^2 \frac{\partial h}{\partial x} + \rho^3 \left(\frac{\partial h}{\partial x} \right)^2 + \dots \quad (\text{B5})$$

In the absence of any drift velocity, the equation of motion of $h(x, t)$ is diffusive.

$$\frac{\partial h}{\partial t} = \Gamma' \frac{\partial^2 h}{\partial x^2} + \eta(x, t). \quad (\text{B6})$$

The noise term $\eta(x, t)$ is Gaussian: $\langle \eta(x, t) \rangle = 0$, $\langle \eta(x, t) \eta(x', t') \rangle = 2A \delta(x - x') \delta(t - t')$.

In the presence of a drift velocity $v(x, t)$, an additional term $v(x, t)$ appears on the rhs of the above equation. The drift velocity depends on x and t only through the local density $\rho(x, t)$ which is the only possibility in the coarse-grained lattice gas. Thus $v(x, t) = v(\rho(x, t))$. We now substitute $\rho(x, t) = \rho + \psi(x, t)$ and expand in a power series in $\psi(x, t)$.

$$v(x, t) = v(\rho) + \left[\frac{\partial v}{\partial \rho} \right]_{\rho} \psi(x, t) + \frac{1}{2} \left[\frac{\partial^2 v}{\partial \rho^2} \right]_{\rho} \psi^2(x, t) + \dots \quad (\text{B7})$$

Thus, we get

$$\begin{aligned} \frac{\partial h}{\partial t} &= v(\rho) + \Gamma' \frac{\partial^2 h}{\partial x^2} - \rho^2 \left[\frac{\partial v}{\partial \rho} \right]_{\rho} \frac{\partial h}{\partial x} + \frac{1}{2} \left[\frac{\partial^2 v}{\partial \rho^2} \right]_{\rho} \rho^4 \left(\frac{\partial h}{\partial x} \right)^2 \\ &+ \left[\frac{\partial v}{\partial \rho} \right]_{\rho} \rho^3 \left(\frac{\partial h}{\partial x} \right)^2 + \dots + \eta(x, t) \quad (\text{B8}) \\ &= v(\rho) + \Gamma' \frac{\partial^2 h}{\partial x^2} + u' \frac{\partial h}{\partial x} + \frac{\lambda'}{2} \left(\frac{\partial h}{\partial x} \right)^2 + \dots + \eta(x, t). \end{aligned} \quad (\text{B9})$$

Here, $v(\rho)$ is the mean drift velocity of the particle and hence, equals v_P in our notation. Also, $u' = \rho \left[v(\rho) - \frac{\partial J}{\partial \rho} \right]_{\rho}$ where $J(\rho) = \rho v(\rho)$ is the mean current. In terms of the kinematic wave speed v_K , we have $u' = \rho(v_P - v_K)$. The nonlinearity coefficient $\lambda' = \rho^3 \left[\frac{\partial^2 J}{\partial \rho^2} \right]_{\rho}$. Note that x in the above equation stands for the tag variable in the continuum. Now, dividing x by the particle density ρ to make it into a spatial variable, we finally get from Eq. B9, to lowest order of nonlinearity,

$$\frac{\partial h}{\partial t} = v_P + \Gamma \frac{\partial^2 h}{\partial x^2} + u \frac{\partial h}{\partial x} + \frac{\lambda}{2} \left(\frac{\partial h}{\partial x} \right)^2 + \eta(x, t), \quad (\text{B10})$$

where

$$u = v_P - v_K, \quad (\text{B11})$$

while

$$\lambda = \rho \left[\frac{\partial^2 J}{\partial \rho^2} \right]_{\rho}. \quad (\text{B12})$$

Using $J(\rho) = (p - q)\rho(1 - \rho)$ and $v_P = (p - q)(1 - \rho)$ for the ASEP, we get

$$u = \rho(p - q), \quad (\text{B13})$$

$$\lambda = -2\rho(p - q). \quad (\text{B14})$$

Utilizing the above expressions for u and λ in Eq. B10, we get the time evolution equation for the interface equivalent to the ASEP, Eq. 7.

Expressions for the coefficients Γ and A in terms of microscopic parameters can be found by setting $p = q = 1/2$, in which case the ASEP reduces to the SEP. The coefficient Γ can then be calculated explicitly [42, 43], with the result

$$\Gamma = \frac{1}{2}. \quad (\text{B15})$$

Further, Eq. B10 reduces to the EW equation, Eq. 8, and $\sigma^2(t)$ can be found from Section V by considering the limit $u \rightarrow 0$. The result is $\sigma^2(t) \approx \frac{2A}{\sqrt{\pi}\Gamma} \sqrt{t}$. Comparing with the exact result $\sigma^2(t) \approx \sqrt{\frac{2}{\pi}} \left(\frac{1-\rho}{\rho} \right) \sqrt{t}$ for the SEP [1], one gets $\frac{A}{\sqrt{\Gamma}} = \frac{1}{\sqrt{2}} \left(\frac{1-\rho}{\rho} \right)$. Using Eq. B15, we finally get

$$A = \frac{1}{2} \left(\frac{1-\rho}{\rho} \right). \quad (\text{B16})$$

APPENDIX C: EVALUATION OF THE INTEGRAL $\int_{k=0}^{\infty} \frac{dk}{k^2} [1 - e^{-ck^2} \cos(k)]$

Let

$$I(c) = \int_{k=0}^{\infty} \frac{dk}{k^2} [1 - e^{-ck^2} \cos(k)]. \quad (\text{C1})$$

Thus,

$$\frac{dI}{dc} = \int_{k=0}^{\infty} dk e^{-ck^2} \cos(k) = \frac{1}{2} \sqrt{\frac{\pi}{c}} e^{-1/4c}. \quad (\text{C2})$$

Also, $I(0) = \frac{\pi}{2}$. Hence,

$$I(c) = \frac{\pi}{2} + \frac{1}{2} \int_0^c dx \sqrt{\frac{\pi}{x}} e^{-1/4x}. \quad (\text{C3})$$

Doing the integral on the rhs by parts, we finally get

$$I(c) = \frac{\pi}{2} + \sqrt{\pi c} e^{-1/4c} - \frac{\sqrt{\pi}}{2} \int_{1/4c}^{\infty} dy e^{-y} y^{-1/2}. \quad (\text{C4})$$

Using the usual definition of the complementary error function, $\text{erfc}(z) = \frac{2}{\sqrt{\pi}} \int_z^{\infty} dt e^{-t^2} = 1 - \text{erf}(z)$, (where

$\text{erf}(z)$ is the usual error function), we can rewrite the above expression as

$$I(c) = \frac{\pi}{2} + \sqrt{\pi c} e^{-1/4c} - \frac{\pi}{2} \text{erfc}\left(\frac{1}{2\sqrt{c}}\right) \quad (\text{C5})$$

$$= \sqrt{\pi c} e^{-1/4c} + \frac{\pi}{2} \text{erf}\left(\frac{1}{2\sqrt{c}}\right).$$

-
- [1] T. M. Liggett, *Interacting Particle Systems* (Springer-Verlag, New York, 1985).
- [2] A. De Masi and P. A. Ferrari, *J. Stat. Phys.* **38**, 603 (1985); R. Kutner and H. van Beijeren, *J. Stat. Phys.* **39**, 317 (1985).
- [3] B. Derrida, M. R. Evans, and D. Mukamel, *J. Phys. A: Math. Gen.* **26**, 4911 (1993); B. Derrida and K. Mallick, *J. Phys. A: Math. Gen.* **30**, 1031 (1997).
- [4] H. van Beijeren, *J. Stat. Phys.*, **63**, 47 (1991).
- [5] S. N. Majumdar and M. Barma, *Phys. Rev. B* **44**, 5306 (1991).
- [6] S. N. Majumdar and M. Barma, *Physica A* **177**, 366 (1991).
- [7] In the absence of the external drive, it is known that $\sigma^2(L, t) \sim t^{1/2}$ [T. E. Harris, *J. Appl. Probab.* **2**, 323 (1965); R. Arratia, *Ann. Probab.* **11**, 362 (1983); see also Ref. [1]]. In the ASEP, if the external drive is small, there is a size-independent short-time precursor to the initial linear regime where $\sigma^2(L, t) \sim t^{1/2}$.
- [8] M. J. Lighthill and G. B. Whitham, *Proc. R. Soc. London A* **229**, 281 (1955).
- [9] M. J. Lighthill and G. B. Whitham, *Proc. R. Soc. London A* **229**, 317 (1955).
- [10] D. Chowdhury, L. Santen, and A. Schadschneider, *Phys. Rep.* **329**, 199 (2000) Section 4.1.
- [11] J. Lee, *Phys. Rev. E* **49**, 281 (1994).
- [12] M. Barma, *J. Phys. A: Math. Gen.* **25**, L693 (1992).
- [13] M. Barma, in *Non Linear Phenomena in Materials Science III - Instabilities and Patterning*, edited by G. Ananthakrishna, L. P. Kubin, and G. Martin (Scitec Publications, Untermüli, 1995).
- [14] M. Barma and R. Ramaswamy, in *Non-Linearity and Breakdown in Soft Condensed Matter*, edited by K. K. Bardhan, B. K. Chakrabarti, and A. Hansen (Springer-Verlag, Berlin, 1994).
- [15] M. Kardar, G. Parisi, and Y. C. Zhang, *Phys. Rev. Lett.* **56**, 889 (1986).
- [16] S. Katz, J. L. Lebowitz, and H. Spohn, *Phys. Rev. B* **28**, 1655 (1983); (b) *J. Stat. Phys.* **34**, 497 (1984).
- [17] J. Krug and J. Garcia, *J. Stat. Phys.* **99**, 31 (2000); R. Rajesh and S. N. Majumdar, *J. Stat. Phys.* **99**, 943 (2000).
- [18] D. Kim, *Phys. Rev. E* **52**, 3512 (1995); O. Golinelli and K. Mallick, *J. Phys. A: Math. Gen.* **38**, 1419 (2005).
- [19] Note that there are other mappings of ASEP to an interface that have their own merits, e.g., Ref. [1]; M. Plischke, Z. Racz, and D. Liu, *Phys. Rev. B* **35**, 3485 (1987). Here, one identifies the presence of a particle with a downward slope of the interface while the absence of a particle is identified with an upward slope. In this way, the ASEP density profile maps onto a nonequilibrium interface, described by the KPZ equation.
- [20] S. F. Edwards and D. R. Wilkinson, *Proc. R. Soc. London, Ser A* **381**, 17 (1982).
- [21] A. -L. Barabasi and H. E. Stanley, *Fractal Concepts in Surface Growth* (Cambridge University Press, Cambridge, 1995).
- [22] J. M. Hammersley, in *Proceedings of the fifth Berkeley Symposium on Mathematical Statistics and Probability*, edited by L. M. Le Cam and J. Neyman (University of California Press, Berkeley, 1967).
- [23] B. Derrida, J. L. Lebowitz, E. R. Speer, and H. Spohn, *Phys. Rev. Lett.* **67**, 165 (1991); (b) *J. Phys. A*, **24**, 4805 (1991).
- [24] M. Paczuski, M. Barma, S. N. Majumdar, and T. Hwa, *Phys. Rev. Lett.* **69**, 2735 (1992).
- [25] P. M. Binder, M. Paczuski and M. Barma, *Phys. Rev. E* **49**, 1174 (1994).
- [26] B. Subramanian, G. T. Barkema, J. L. Lebowitz and E. Speer, *J. Phys. A: Math. Gen.* **29**, 7475 (1996).
- [27] F. J. Alexander, S. A. Janowsky, J. L. Lebowitz, and H. van Beijeren, *Phys. Rev. E* **47**, 403 (1993).
- [28] D. Dhar, *Phase Transitions* **9**, 51 (1987); L. -H. Gwa and H. Spohn, *Phys. Rev. A* **46**, 844 (1992).
- [29] G. Tripathy and M. Barma, *Phys. Rev. Lett.* **78**, 3039 (1997).
- [30] D. Das, A. Basu, M. Barma and S. Ramaswamy, *Phys. Rev. E* **64**, 021402 (2001).
- [31] A. A. Ferreira and F. C. Alcaraz, *Phys. Rev. E* **65**, 052102 (2002).
- [32] J. M. Luck, C. Godrèche, *J. Stat. Mech.* P08009 (2006).
- [33] M. R. Evans and T. Hanney, *J. Phys. A: Math. Gen.* **38** R195 (2005).
- [34] C. Godrèche, cond-mat/0603249; also, *Lecture Notes in Physics 716*, (Springer-Verlag, 2007).
- [35] F. Kelly, *Reversibility and Stochastic Networks* (Wiley, Chichester, 1979).
- [36] C. Godrèche and J. M. Luck, *J. Phys. A: Math. Gen.* **36**, 9973 (2003).
- [37] R. Rajesh and S. N. Majumdar, *Phys. Rev. E* **64**, 036103 (2001).
- [38] H. van Beijeren, R. Kutner, and H. Spohn, *Phys. Rev. Lett.* **54**, 2026 (1985).
- [39] G. B. Whitham, *Linear and Nonlinear Waves* (John Wiley & Sons, New York, 1974).
- [40] G. M. Schütz in *Phase Transitions and Critical Phenomena 19*, edited by C. Domb and J. L. Lebowitz (Academic, London, 2001) Section 4.2.2.
- [41] S. N. Majumdar, Ph. D. Thesis (Bombay University) (1992) (unpublished).
- [42] R. Kutner, *Phys. Lett.* **81A**, 239 (1981).
- [43] R. B. Stinchcombe, M. D. Grynberg, and M. Barma, *Phys. Rev. E* **47**, 4018 (1993).